

# **GEOLOGY FOR SOCIETY**

SINCE 1858



**GEOLOGICAL  
SURVEY OF  
NORWAY**

· NGU ·



<b>Report no.:</b> 2018.021		<b>ISSN: 0800-3416 (print)</b> <b>ISSN: 2387-3515 (online)</b>		<b>Grading:</b> Open	
<b>Title:</b> Assessment of AUV-borne acoustic and optical sensors for seabed and biotope mapping in MAREANO					
<b>Authors:</b> Terje Thorsnes, Pål Buhl-Mortensen, Øyvind Tappel, Frank Jakobsen, Kjetil Tesaker Olsen, Gjertrud Jensen, Lilja Rún Bjarnadóttir and Hanne Hodnesdal			<b>Client:</b> MAREANO		
<b>County:</b> Nordland			<b>Commune:</b>		
<b>Map-sheet name (M=1:250.000)</b>			<b>Map-sheet no. and -name (M=1:50.000)</b>		
<b>Deposit name and grid-reference:</b>			<b>Number of pages:</b> 48		<b>Price (NOK):</b> 140
			<b>Map enclosures:</b>		
<b>Fieldwork carried out:</b> 15.10.-20.10.2015		<b>Date of report:</b> 7.9.2018		<b>Project no.:</b> 311721	
			<b>Person responsible:</b> Reidulv Bøe <i>Reidulv Bøe</i>		
<b>Summary:</b> <p>MAREANO (NGU, Kartverket and HI) in collaboration with FFI conducted a survey using the autonomous underwater vessel (AUV) HUGIN HUS to assess the suitability and advantages of AUV-borne acoustic and optical tools for seabed and biotope mapping. Due to poor weather conditions, the first part of the cruise was carried out in Andfjorden, Nordland. The second part was carried out in the main target area of Vesterdjupet, Nordland. Both acoustic and optical data collection were affected by technical problems which reduced the data quality.</p> <p>Acoustic and optical data collected with the HUGIN HUS AUV were compared with acoustic data from surface vessels, and data from the standard MAREANO towed video system Campod. The analyses show a clear potential for using AUVs in MAREANO, but also clear limitations. Some of the limitations have been overcome by drastic improvements of the AUV technology since 2015.</p>					
<b>Keywords:</b> AUV		Synthetic aperture sonar		EM2040	
Subbottom profiler		Seabed mapping		TFish	
Biotope mapping		Sediment map		Coral reef damage	

# CONTENTS

1. INTRODUCTION.....	4
2. METHODS.....	5
2.1 Hullborne multibeam bathymetry .....	5
2.2 Autonomous Underwater Vehicle (AUV) borne methods.....	5
2.2.1 AUV-borne acoustic methods .....	10
2.2.2 AUV-borne optical and chemical methods.....	12
3. PLANNED SURVEY AREAS.....	13
4. OPERATIONS.....	16
4.1 Andfjorden.....	16
4.2 Vesterdjupet.....	19
5. GEOLOGICAL AND BATHYMETRIC INFORMATION FROM HULLBORNE VERSUS AUV-BORNE PLATFORMS .....	21
5.1 Technical analysis of bathymetry from EM710, EM2040 and HiSAS 1030 .....	21
5.2 Visual analysis of bathymetry, backscatter and imagery from EM710, EM2040 and HiSAS 1030.....	25
5.3 Image quality and suitability for geological mapping - Campod and TFish images .	32
5.4 Geological map production based on Campod versus TFish .....	33
6. COMPARISON OF SPECIES COMPOSITION AND BIODIVERSITY BETWEEN AUV STILLS AND CAMPOD VIDEOS .....	38
7. USING AUV-BASED SENSORS FOR CORAL MONITORING .....	43
8. CONCLUSIONS .....	44
9. APPENDIX .....	47
10. REFERENCES .....	48



## 1. INTRODUCTION

Since 2005, hullborne (surface) multibeam echosounders, towed high-definition video system and physical ground truthing have been the main tools for data acquisition for sediment and biotope mapping in MAREANO ([www.mareano.no](http://www.mareano.no)). During the last decade, new options for data acquisition have become widely accessible. The development of AUVs, new acoustic tools such as synthetic aperture sonars, and improved imaging from AUVs offer new possibilities.

AUVs have a wide range of applications in marine geoscience and are increasingly used in the scientific, military, commercial and policy sectors. They have revolutionized the ability to image the seafloor, providing higher resolution data than can be achieved from surface vessels, particularly in deep water (Wynn et al., 2014). The extent and speed of marine environmental mapping is increasing quickly with technological advances, particularly with optical imaging from AUVs (Morris et al. 2014). This is the background for the current method development project financed by MAREANO, aiming at giving a first assessment of the feasibility of including these tools in the MAREANO tool box for data acquisition. This study addresses the following aspects:

1. Assess the suitability of AUV-borne sensors (EM2040 multibeam bathymetry and backscatter, HiSAS 1030 sonar imagery and bathymetry, and TFish colour photo system) for geological seabed mapping and compare this with seabed sediment maps produced using standard MAREANO platforms and sensors.
2. Assess the suitability of the TFish system to identify macrofauna and compare this to the standard MAREANO platform and sensors, compare biotope maps (nature type maps) made using the existing MAREANO methodology and maps made using data only from the AUV. This includes the geological maps used for nature type map production.

The original goals of the study included comparison of biotope maps produced using the traditional and new methods, assessment of the suitability of AUV-borne sensors for “monitoring criteria” such as percentage of live corals, a more thorough comparison of hullborne and AUV-borne bathymetry, and an assessment of the potential use within biotope mapping, including a cost/benefit analysis. Due to challenges during the field campaign with weather conditions leading to a reduced data set, and limited resources for interpretation and reporting, it has not been possible to address these goals in full scale.

Data have been collected from two areas - Andfjorden and Vesterdjupet west of Røst, Lofoten. These areas may not be ideal for using AUVs, because the topography is partly rugged (AUVs is best suited for wide, flat areas). The planning of routes for AUV data collection was steered by the existence of video lines collected by the MAREANO program. This report describes how data were collected and operational aspects of data acquisition using a suite of hullborne and AUV-borne instruments. Due to limited resources for

interpretation and reporting, and data confidentiality for the Andfjorden data, only the results from Vesterdjuvet are reported here.

## **2. METHODS**

A multitude of instruments mounted on two different platforms was involved to address the aspects outlined in the previous chapter. Conventional multibeam bathymetry, backscatter and water column data were collected from the surface vessel H.U. Sverdrup II (chapter 2.1). The HUGIN HUS AUV was used as platform for a Kongsberg EM2040 multibeam echosounder, a HiSAS 1030 synthetic aperture sonar, a TFish colour imagery system, an EdgeTech 2200 subbottom profiler, and a Franatech methane sniffer, along with standard environmental sensors for temperature, salinity and turbidity (chapter 2.2). In addition, the optical imagery data were compared with previously acquired optical data collected using the standard MAREANO video system (Campod) and instruments thereon (chapters 5.3 and 5.4).

### **2.1 Hullborne multibeam bathymetry**




Hullborne multibeam bathymetry echosounder (MBE) data were collected using EM710 in two areas of Andfjorden with variable topography. Existing data from the MAREANO programme were used in Vesterdjuvet together with new data which included water column data. The operating frequency used by EM710 is 70-100 kHz which is advantageous for the intermediate water depths between 200 m and 1000 m, where other systems usually need a change in frequency. The water column data recorded by the system can be used for detection of active gas seeps and biological objects in the water column. CARIS was used onboard to process the bathymetry data. Backscatter data were processed using Fledermaus GeoCoder Tool. FlederMaus Midwater package was used to process water column data for detecting gas anomalies.

### **2.2 Autonomous Underwater Vehicle (AUV) borne methods**

HUGIN HUS is an AUV from Kongsberg (HUS is abbreviation for H.U. Sverdrup, and is the name of the HUGIN owned by FFI). The AUV is a one-of-a-kind experimental research AUV, with several modifications. This includes possibility to change the angle of the HiSAS RX array, using the EM2040 in an upward-looking mode, and using non-standard sensors. The AUV is 5.6 m long, with a diameter of 0.75 m, a dry weight of 1000 kg and can operate down to 3000 m depth. The AUV is normally launched from the stern of the ship, where it is stored and maintained in a dedicated container (figure 1a). It is equipped with inertial navigation and HiPap positioning from the mothership. The HUGIN was flown at different heights depending on the purpose – acoustic or optical data acquisition. For minimum sensor use and low speed the HUGIN can operate over 24 hours before birthing to mothership. If

multiple sensors are in use, the operation time is about 12 hours. For a chosen HUGIN version each sensor onboard is pressure tested for a specified depth area. HUGIN comes with both 1000 m, 3000 m and 4500 m operational depth options (table 1). For more information, see Appendix 9.1.

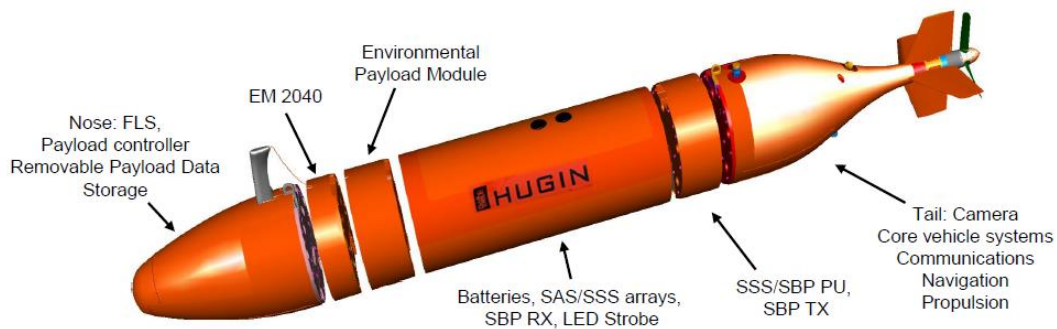
**Table 1. HUGIN family standard specifications. The HUGIN HUS is an experimental research AUV, with several modifications.**

	HUGIN 1000	HUGIN 1000 for 3000 m	HUGIN 3000	HUGIN 4500
Weight	650-850 kg	650-850 kg	1400 kg	1900 kg
Length	4.5 m	4.7 m	5.5 m	6.0 m
Diameter	0.75 m	0.75 m	1.00 m	1.00 m
Speed	2-6 kts	2-6 kts	2-4 kts	2-4 kts
Depth	1000 m	3000 m	3000 m	4500 m
Battery	LiPolymer pressure tolerant. 15 KWh	LiPolymer pressure tolerant. 15 KWh	Al/HP semi fuel cell, 45 KWh	Al/HP semi fuel cell, 60 KWh
Endurance	24hrs @ 4kts (with MBE, SSS, SBP and CTD)	24hrs @ 4kts (with MBE, SSS, SBP and CTD)	60hrs @ 4kts (with MBE, SSS, SBP and CTD)	60hrs @ 4kts (with MBE, SSS, SBP and CTD)
Navigation system and sensors (main + options)	NavP AINS: IMU, DVL, Depth, USBL, NavP TP Ranging, GPS, TerrNav	NavP AINS: IMU, DVL, Depth, USBL, NavP TP Ranging, GPS, TerrNav	NavP AINS: IMU, DVL, Depth, USBL, NavP TP Ranging, GPS, TerrNav	NavP AINS: IMU, DVL, Depth, USBL, NavP TP Ranging, GPS, TerrNav
Communication (main + options)	Acoustic command and data links, RF, Iridium, Ethernet, WLAN	Acoustic command and data links, RF, Iridium, Ethernet, WLAN	Acoustic command and data links, RF, Iridium, Ethernet, WLAN	Acoustic command and data links, RF, Iridium, Ethernet, WLAN
Payloads (main + options)	MBE, SSS, SBP, SAS, CTD turbidity sensor, ADCP, camera+ others	MBE, SSS, SBP, CTD turbidity sensor, ADCP, camera + others	MBE, SSS, SBP, CTD ADCP, camera + others	MBE, SSS, SBP, CTD, ADCP + others
Main applications	Naval, research, offshore, hydrography	Naval, research, offshore, hydrography	Offshore, research	Offshore, research
				

HUGIN can operate autonomously if needed with aid from surface vessel, using USBL (HiPAP), inertial, DVL and density systems. All HUGIN platforms are delivered with NavLab software. For more information, see Appendix 9.2.



## HUGIN AUV System



### Key Navigation System Components



IHO Quality positioning ensures data relevance

Figure 1. A: Launch of the AUV from its container, at the stern of H.U. Sverdrup II (Photo: Terje Thorsnes). B: Payload of the HUGIN HUS AUV.

The following payloads are described in this document:

- HiSAS 1030 synthetic aperture sonar (SAS arrays in figure 1b) (2.2.1)
- EM2040 multibeam echosounder custom for HUGIN. (2.2.1)
- EdgeTech 2200 sub bottom profiler (SBP in figure 1b) (2.2.1)
- TFish colour imagery system (see 2.2.2)
- Franatech Methane sniffer (2.2.2)
- Standard environmental sensors (salinity, temperature, turbidity) (2.2.2)

For more information about the payload see Appendix 9.3.

An overview of flight heights and resolution is given in table 2.



**Table 2: Sensors on HUGIN.**

Sensor	Min flight height	Max flight height	Optimal flight height	Width and resolution when using optimal flight height	Argument for choosing optimal flight height
HiSAS 1030	7 - 8 m (*)	50m (*)	20 - 25 m (*)	2 x 180 m, 2 cm (speed dependent). Image 10 x 10 cm and bathymetry 20 x 20 cm. (*)	Combination of HiSAS 1030 and MBES to achieve optimal bathymetric coverage. (**)
EM2040 0.7° x 0.7° (**)	2 - 3 m (**)	150 m (**)	40 – 50 m (*) Separate run. (20 - 25 m in combination with HiSAS 1030) (*)	90 – 100 m swath width (coverage sector of 120°). 0.5 m resolution (*)	Combination of HiSAS 1030 and MBES to achieve optimal bathymetric coverage. (**)
EdgeTech 2200	4 m (*)	50 m (*)	5 – 20 m (*)	Center beam (2D data)	
TFish	Safety dependent	10 m	3 – 5 m	4 m, 0.2 cm	Light and water turbidity
Franatech Methane sniffer	2 - 3 m (*)	50 m (*)	5 – 20 m (*)		Gas flares dissolve away from seabed
Standard environmental sensors	Diverse	Diverse	Diverse	Sound speed calculated from CTD.	

(\*) - based on operational experiences. (\*\*) – based on conservative estimates from supplier.

### 2.2.1 AUV-borne acoustic methods

HiSAS 1030 is a high resolution interferometric synthetic aperture sonar system with frequency 85-115 kHz, capable of providing very high resolution images and detailed bathymetry of the seabed. The system has a range-independent resolution of typically 4x4 cm (maximum 2x2 cm) out to a distance of 170 m from both sides of the AUV at a speed of 2 m/s. For further details – see Appendix 9.4.

The data were processed onboard. Raw, unprocessed sidescan sonar data in xtf format were ready within a few hours. Processed high resolution mosaics in geotiff format were available for inspection in Reflection and/or ArcMap within 10 hours of HUGIN recovery.

Multibeam echo sounder data were collected by HUGIN using the Kongsberg EM2040 system, with 200/300/400 kHz frequency. Data were stored in .all format for further processing of bathymetry and backscatter using CARIS and Fledermaus GeoCoder. The EM2040 transducer had accidentally been rotated 180° during mounting on the AUV. This meant that extensive reprocessing by Kongsberg Maritime and FFI was required. The quality of the reprocessed data is considered as acceptable, but not as good as it could have been. Normally we would expect to have a first gridding and backscatter mosaic ready within a few hours of data extraction from the AUV.

A combination of HiSAS 1030 and EM 2040 is often used to optimize bathymetry coverage. In such cases, the AUV operates 20 m above the seafloor for bathymetric purposes (figure 2). For more information, see Appendix 9.5.

Processing was done with NavLab software. This workflow of this is not be evaluated in this report. FFI have done this work, both in NavLab and inhouse software.

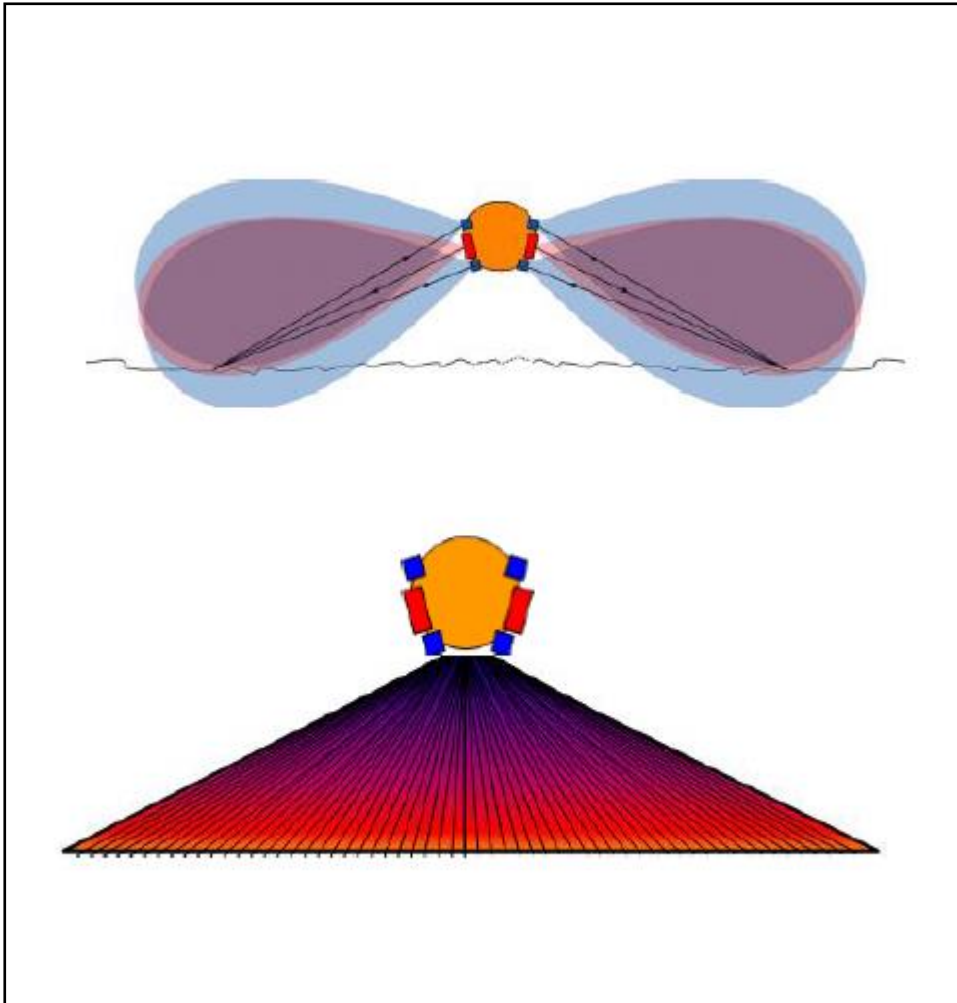


*Figure 2. Illustrating the complimentary coverage of a HiSAS 1030 system and a EM2040 system. Front view.*

The HUGIN can be used for reconnaissance survey and is not dependant on surface-based survey before AUV operations. However, for planning purposes, surface-based survey data can document areas of interest. When operating close to the seabed (<3 m above the seabed) in shallow and medium water depths, surface-based bathymetry with resolution better than 3 x 3 m is highly recommended. This is due to risk of collision and for manoeuvring up steep slopes. The practical depth limit for this resolution when using surface-based vessels is about 500 m. According to Kongsberg Maritime the HUGIN is equipped with avoidance sonar.

The EdgeTech 2200 is a high resolution subbottom profiler (SBP) with several pulse types. The frequency spectrum is 2 – 12 kHz, giving 5 – 20 ms pulse width. At 10 m flight height, the vertical resolution is less than 100 milliseconds (ca. 10 cm). The penetration depends on the sediments. The EdgeTech data are available to the user as jsf files, which may be converted to segy files.

### 2.2.2 AUV-borne optical and chemical methods

The TFish electro-optical colour imagery system was a one-of-a-kind prototype developed by FFI and Norsk Elektrooptikk. There were several issues with it, and it is no longer in use. The camera has a native resolution of 4008x2672, but usually some pixels are “added up” to increase light sensitivity. The typical trade-off (resolution vs range) image resolution for colour images are 2004x1336. The field of view is approximately equal to flight height, giving a pixel size of 0.35 x 0.35 cm at 7 m flight height. The TFish images were available co-registered with the HiSAS 1030 data within hours of HUGIN recovery through the Reflection software system onboard HU Sverdrup II, but the quality of the images was generally poor due to problems with colour calibration. FFI reprocessed the images to an acceptable quality.

The Franatech Methane Sniffer (METS) has a methane sensitive detector located in a detector room in the sensor head. The detector room is protected against water and pressure by a silicone membrane. The gas molecules diffuse through the membrane, following the partial pressure gradient between water and detector room, according to Henry’s law. Hence, the concentration in the detector room is directly correlated to the concentration in the outside water. The sensitivity in the pumped flow-through mode is 1 nM – 500 nM. The reaction time is within a few seconds (METS product sheet, from [www.franatech.com](http://www.franatech.com)). The T90 time (time to reach 90% of the end-value) for this version of METS is typically within 5 min in pumped-through mode (Michel Masson, Franatech – pers comm.). Data set deliveries included GeoTiff files and ASCII text files. Data set deliveries from the environmental sensors included GeoTiff files and ASCII text files.



### 3. PLANNED SURVEY AREAS

The survey areas were selected to address the prioritized goals. These criteria were emphasized:

- Reasonable transit from the port of mobilisation/demobilisation (Svolvær)
- Sufficiently wide range of sediments/ecosystems/biotopes including topographic variation
- include areas with reasonable amount of macrofauna
- well documented bathymetry for planning – suitable for TFish dives, but also HiSAS 1030 and EM2040
- reasonable coverage of MAREANO video lines
- high quality backscatter available

Based on these criteria, two main areas were selected - the Vesterdjupet basin on the continental shelf, and a canyon at 800 m water depth at the continental slope west of Lofoten (figure 3). Two backup areas in case of bad weather were selected in the fjords - Tysfjorden and Andfjorden.

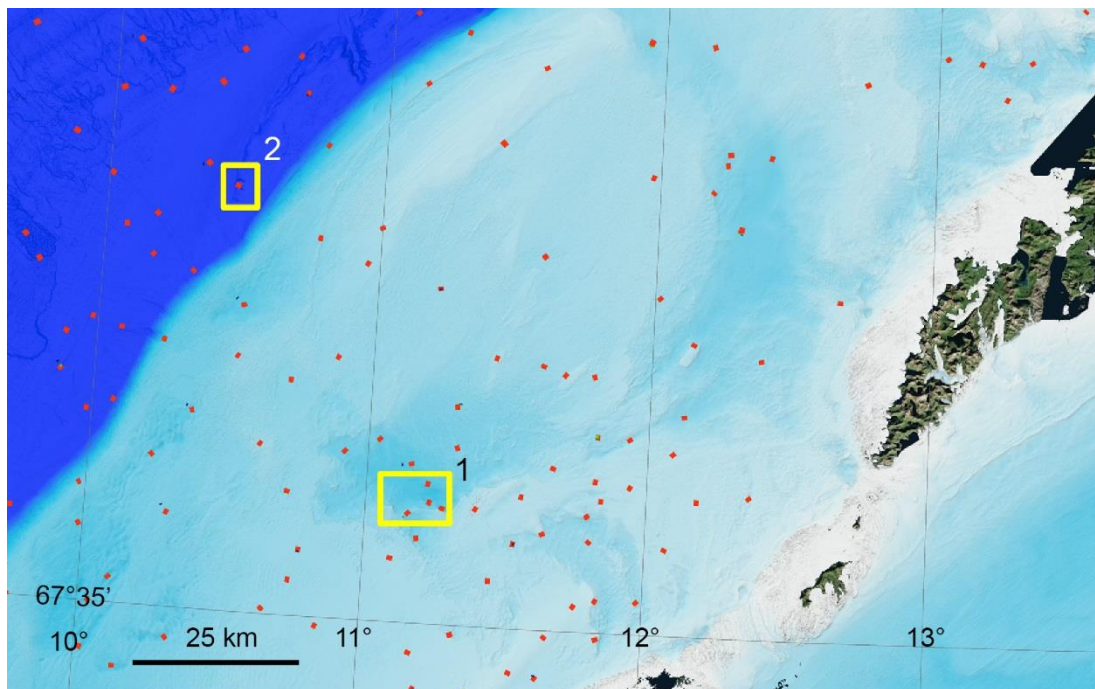


*Figure 3. The two areas selected for data acquisition, west of Lofoten (yellow polygons). Red lines show existing campod lines. 1 - Vesterdjupet basin. 2 - Canyon at 800 m depth on the continental slope.*

### **Area 1 – Vesterdjupet**

The Vesterdjupet basin in the middle of Røstbanken northeast of Trænadjupet (figure 3) is more than 100 m deep and covers an area of around 500 km<sup>2</sup>. The depression is asymmetric - with fairly steep basin boundaries in the southeast (up to 10° - 15°) becoming more gently sloping in the northwest. At the southeastern margin, we also find a bedrock ridge, rising as much as 50 m above the surrounding seabed. The sediments in Vesterdjupet and the immediate vicinity range from sandy mud to gravel, boulders and exposed bedrock. The chosen area (80 km<sup>2</sup>) offers a wide range of geology within a limited area. Four video lines recorded by MAREANO in 2011 were also available. One documented coral reef and several bioclastic mounds (see Bellec et al. 2014, Thorsnes et al. 2015) are present. The area is bound by coordinates 68°7'39" 10°25'6" (lower left corner) and 68°11'16" 10°31'51" (upper right corner).

### **Area 2 – canyon west of Lofoten**

The selected canyon, located at 800 m water depth at the continental slope west of Lofoten (figure 3), is 45 m deep, 200 m wide, 1700 m long and covers an area of around 1 km<sup>2</sup>. The area is bound by coordinates 68°7'39" 10°25'6" (lower left corner) and 68°11'15" 10°31'51" (upper right corner). The area is well suited for comparison of hullborne and AUV-borne bathymetry. A MAREANO video line (R777) crossing the canyon documented probable carbonate crusts, but no gas flares have been observed from the water column of the multibeam bathymetry data.

### **Area 3 - Andfjorden**

Andfjorden was a reserve area in case of bad weather conditions west of Lofoten (areas 1 and 2). Area 3 is located in Andfjorden (figure 4) and is bound by coordinates 69°6'9" 16°7'54" (lower left corner) and 69°11'39" 16°24'56" (upper right corner). The area is characterised by a wide range of sediments from gravelly sand with blocks to mud. The morphology is strongly variable - including a steep bedrock ridge which is 100 m high, 2500 m long and with slopes exceeding 35°, to flat, muddy basins. The four MAREANO video lines show a reasonable rich mega-fauna.

### **Area 4 - Tysfjorden**

Tysfjorden was a reserve area in case of bad weather conditions west of Lofoten (areas 1 and 2). Area 4 in Tysfjorden is bound by coordinates: 68°13'39" 16°5'30" (lower left corner) and 68°16'22" 16°14'56" (upper right corner). Tysfjorden is characterised by shallow irregular areas in the central parts, steep slopes, and an elongated, flat fjord bottom where muddy sediments can be expected. Seabed sediment composition is expected to vary.

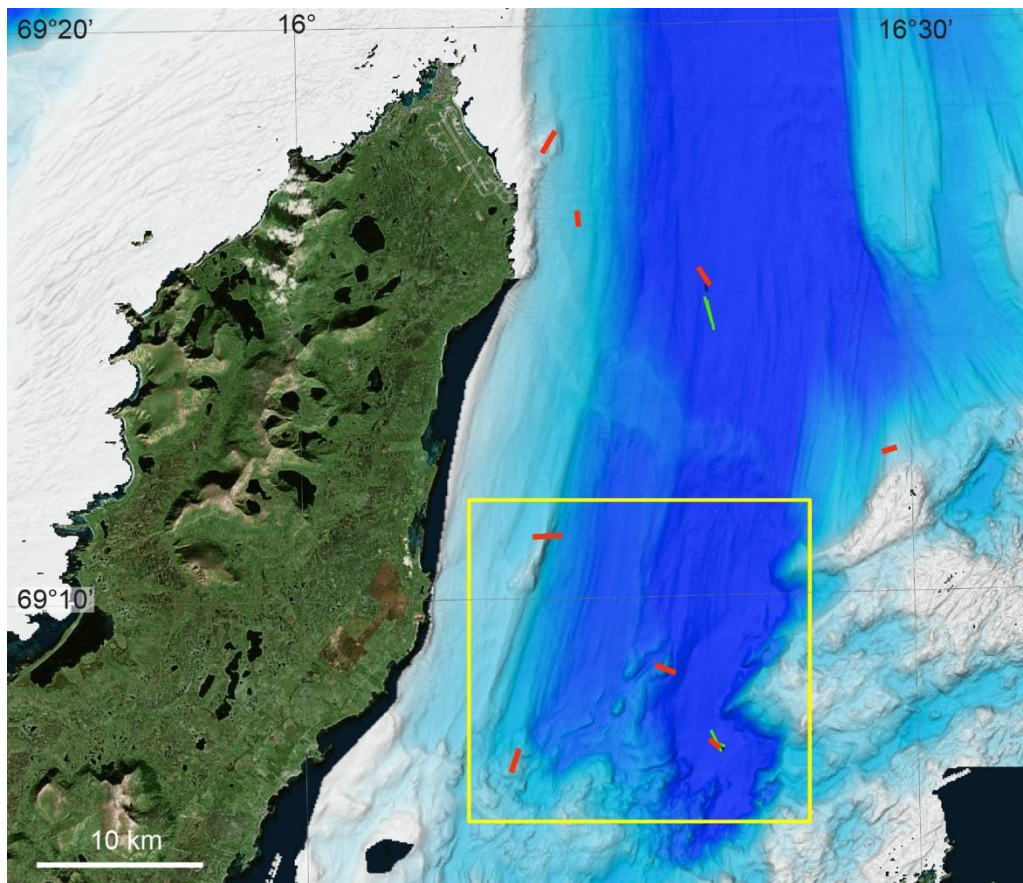


*Figure 4. Planned area for data acquisition in the Andfjorden reserve area (yellow polygon). Red lines show existing campod lines.*

## 4. OPERATIONS

The cruise started from Svolvær 15th October 2015 and ended in Svolvær 20th of October 2015. Due to bad weather, the backup area in Andfjorden was the first area to be investigated. Bad weather causes high waves and vessel motions hindering the recovery of the AUV. It was planned to do grab sampling – this was also hindered by high waves and vessel motions. After three days, the weather calmed, and the last part of the cruise was spent in the Vesterdjuvet area. Maximum sea state for recovery of AUV during operations with HU Sverdrup II is normally 4 to 5. Recharge and download time between recovery and launch was 5 - 6 hours. If two battery sets are available, the turn around time is 30 to 60 minutes.

### 4.1 Andfjorden

In Andfjorden, EM710 multibeam echosounder data were collected first using H.U. Sverdrup II, to provide bathymetry data for planning of the HUGIN operations. Following that, Synthetic aperture imagery and bathymetry, EM2040 multibeam bathymetry and backscatter, and TFish colour photos were collected using HUGIN. The coverage of EM710 backscatter, HiSAS 1030 imagery and location of TFish photos is shown in figure 5.

In the northwestern area and in the transit line towards the southeastern area, HiSAS imagery was acquired at the optimal flight height for HiSAS 1030 (25 m above seabed). EM2040 data and Mets data were collected at the same time, along the same lines. TFish images were acquired during a separate run, with a flight height of 5 - 7 m for capturing images. This proved to be somewhat too high for optimal images.

In the southeastern area, HiSAS 1030 imagery was acquired at the optimal flight height for HiSAS 1030 (25 m above seabed). EM2040 data were collected in a separate run, with the optimal flight height for EM2040 (40 – 50 m above seabed – this is a compromise between resolution and coverage), covering parts of the area where HiSAS 1030 data were collected. TFish images were acquired during a separate run, with a flight height of 5 – 7 m for capturing images. One of the best examples is shown in figure 6. Mets data were collected at the same time.

The EM2040 data had to undergo extensive correction, because the transceiver had been rotated 180° during mounting. This was done by FFI, with assistance from Kongsberg Maritime. The data are graded as confidential, and it is not possible to show geo-referenced results in this report. The same applies for the HiSAS 1030 bathymetry.

The TFish images also had to undergo extensive processing. The geo-referencing of the images did not work properly, and the initial delivery consisted of 14412 jpg images without coordinates. Another severe problem was that the colour balance function was not working



correctly, giving serious problems with the colour profile. FFI post-processed the images, and was able to deliver geotiff (with coordinates) images with a reasonably good colour profile.

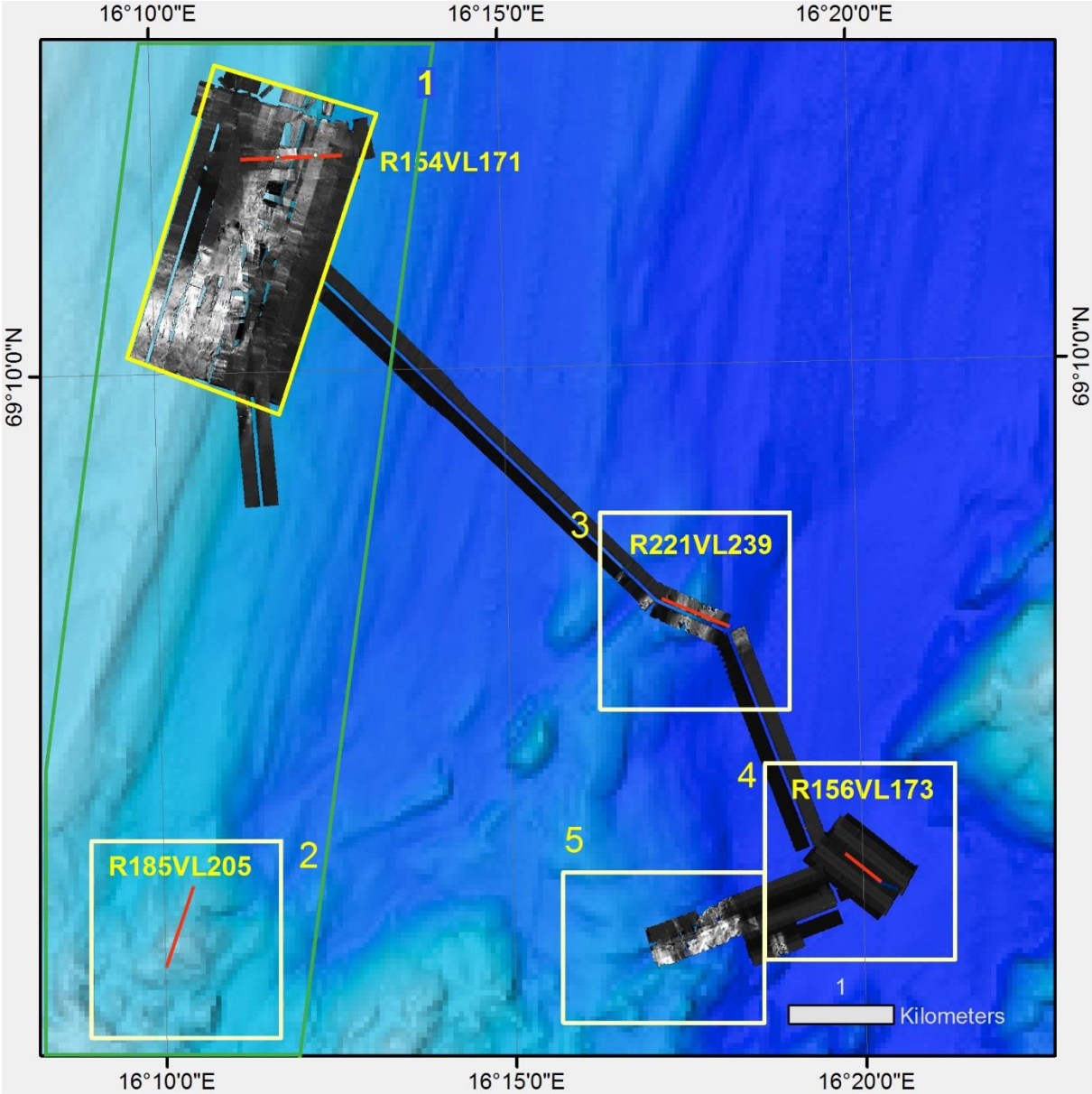
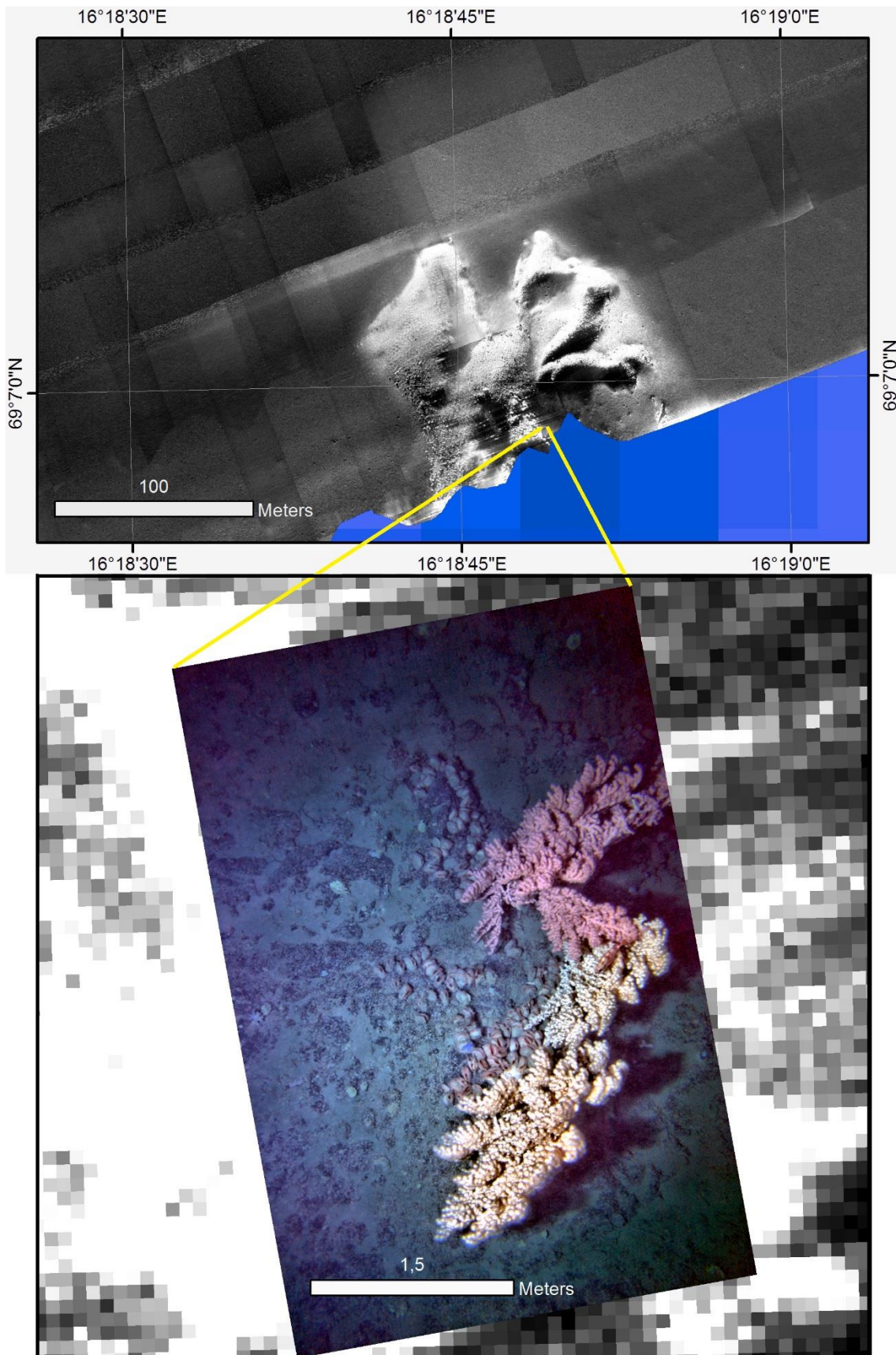


Figure 5. Investigated areas in Andfjorden (1-5), HiSAS 1030 imagery (black – low reflectivity, light grey – high intensity), yellow outline – EM710 coverage, and MAREANO video lines (red).



*Figure 6. Upper panel – HiSAS 1030 sonar imagery showing gravel mound in SW corner of area 4. Lower image – Tfish photo of gravelly seabed with mussels and corals.*

## 4.2 Vesterdjupet

New EM710 multibeam data were first collected in Vesterdjupet. Subsequently, two HUGIN dives were done. The first (Vesterdjupet 151018\_3) started in the evening on the 18<sup>th</sup> October and lasted for nearly 15 hours until the morning on the 19<sup>th</sup> October. The main purpose of this dive was to collect acoustic data. The second dive started in the afternoon on the 19<sup>th</sup> October and lasted for 4 hours until the evening on the same day. Table 3 summarises this.

**Table 3. Overview of data collection.**

Dive	Duration	HiSAS 1030	EM2040	SBP	METS	TFish	Comments
151018_3	15 hours	X	X	X	X		
151019_1	4 hours	X	X	X	X	X	10793 images

The mission plan (figure 7) included:

- 1) 100% HiSAS 1030 sonar imagery and bathymetry coverage (optimized for HiSAS 1030, flying 20-25 m above seabed), EM2040 (20-25 m above seabed), sub-bottom profiling and Mets for the following: a survey line from SW to NE corner of area 4, the whole of area 1, transit to area 5, a line over MAREANO videoline (R751VL779), a transit line to area 2, a line over MAREANO videoline (R796VL824), a transit line to area 3 and a line over MAREANO videoline (R795VL823).
- 2) 200% HiSAS 1030 backscatter and bathymetry coverage (optimised for HiSAS 1030, 20-25 m above seabed) for the western half of area 1.
- 3) Tfish imaging of the video lines in areas 2 (R796VL824), 3 (R795VL823) and 5 (R751VL779) as well as chosen lines in area 1 (between the coral reefs/bioclastic sediment mounds (R752VL780)).
- 4) EM2040 coverage for the western half of area 1 (optimised for EM2040, 40-50 m above the seabed).

Points 1 and 2 were finished successfully. Point 3 was 75% covered, with imaging in all areas except area 3 (the available ship time ended). Point 4 was aborted half way through because of time constraints during dive 151018\_3. The coverage of various data is shown in figure 8.



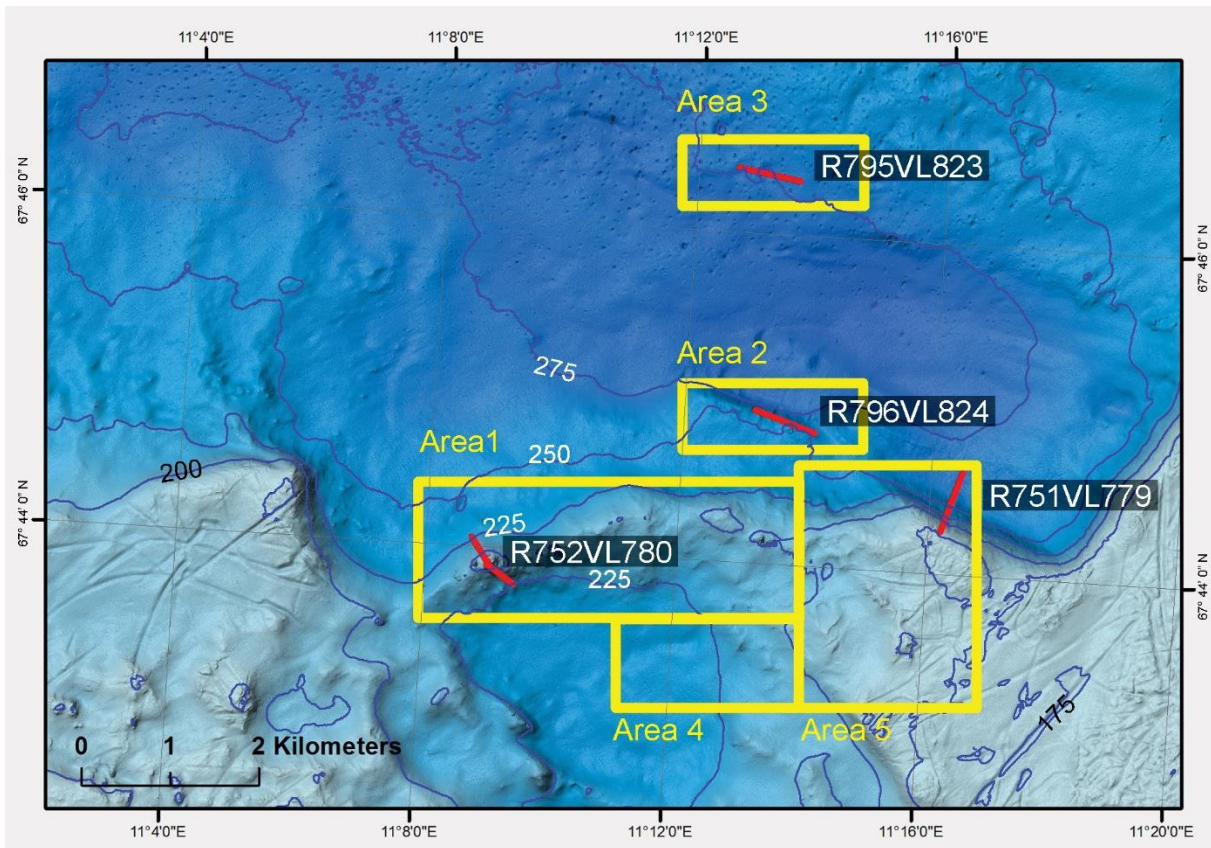


Figure 7. Planned investigated areas in Vesterdjuvet (yellow rectangles), with MAREANO video lines (red).

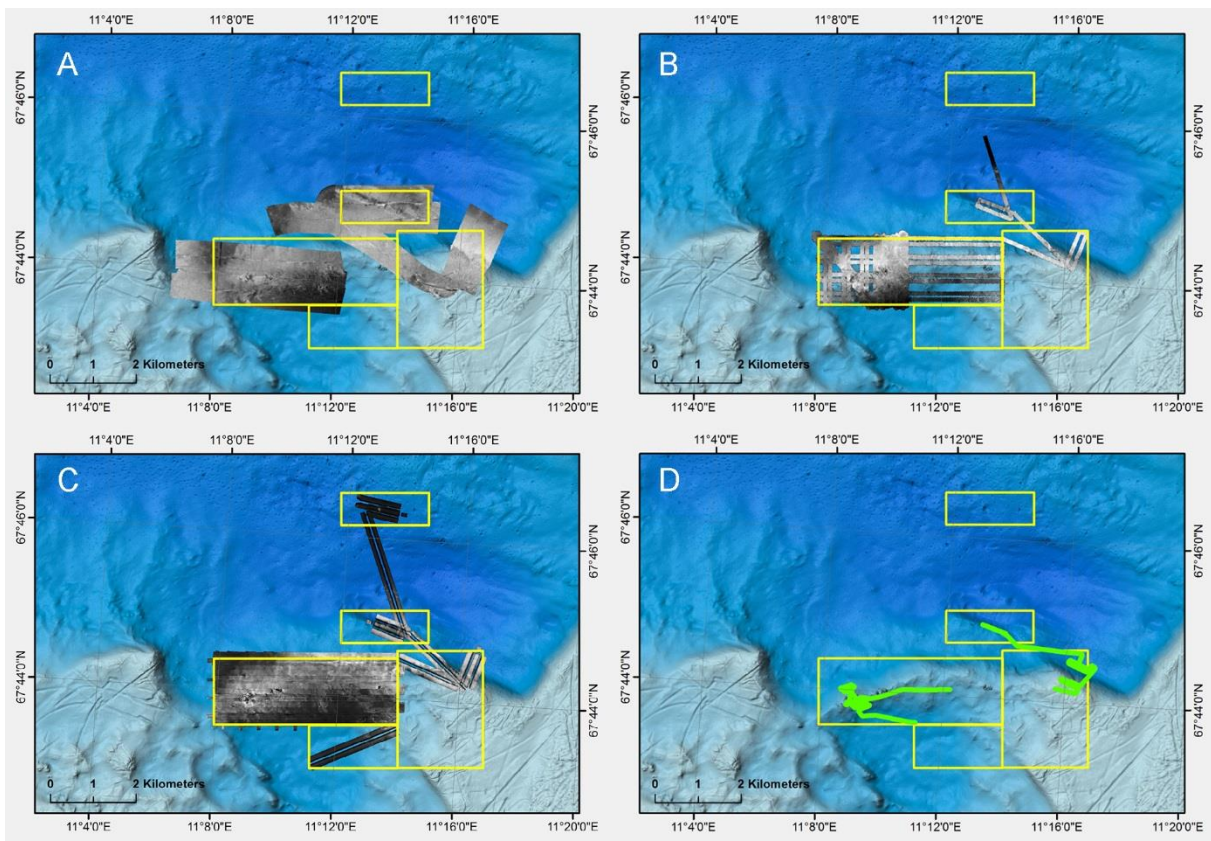


Figure 8. A – ship EM710 coverage. B – AUV EM2040 coverage (backscatter). C – AUV HiSAS 1030 coverage. D – AUV TFish coverage.



## 5. GEOLOGICAL AND BATHYMETRIC INFORMATION FROM HULLBORNE VERSUS AUV-BORNE PLATFORMS

### 5.1 Technical analysis of bathymetry from EM710, EM2040 and HiSAS 1030

Inspection of the data density (figure 9) revealed that the modelling grid size for AUV-borne HiSAS 1030, AUV-born EM 2040 and hullborne EM710 is in the order of 0.2 m, 0.5 m and 3 m, respectively. Hence the HiSAS 1030 data have the highest resolution. Note that the bathymetry data from EM2040 only have partial coverage in the left parts of figure 8b, while the HiSAS 1030 data have full coverage. The reason for this is that the swath width for HiSAS 1030 was c. 300 m, given a flight height of 20-25 m, while the swath width was merely 90-100 m for EM2040 collected simultaneously at swath coverage of 120°. Due to cruise schedule, only the right part of the area was covered with tightly spaced lines allowing full EM2040 coverage.

Looking at a single survey line, the density of the HiSAS 1030 derived bathymetry is approximately 64 points per square meter. The density of the EM 2040 bathymetry is about 20 points per square meter for one single survey line, while the EM 710 only have 0.4 points per square meters (see figure 9 and table 4).

**Table 4. Density of points. 1x1 derived from 3x3.**

Cell 3x3 m	Platform	Nr. of points (est.) 3x3	Nr. of points 1x1
EM 710	HU Sverdrup II	4	0.4
EM 2040	HUGIN	180	20
HiSAS 1030 bathy	HUGIN	760	24

An area with small peaks located on the ridge in area 1 (figure 7) was chosen for further investigation. Level differences within the HiSAS 1030 data are clearly visible in the terrain models (figure 10). The profile (upper panel of figure 10) shows this clearly. The profile shows a stepwise level difference, with a step of 0.4 m and a total level difference of 0.7 m. There are also level differences between the HiSAS 1030 model and the EM 710 model (figure 11). In general, data with internal level differences can mask important features.

The EM 2040 data have a varying degree of internal level differences. In the example in figure 12 the level difference is 1 m. Another issue are lines shifted closer to the surface (0-5 m depth difference). These lines have not been properly processed and are not shown in the figure below.

The synchronization of roll correction was partly off during the mission, due to sensitivity to changes in the roll. This was due to inaccurate time synchronization. This can result in systematic artifacts in the datasets (“ribbing”). See figure 12, dark blue area to the right.

The reason for the step between lines in the HiSAS 1030 data is probably lack of navigation correction or limited navigational accuracy between lines. The software used for extracting bathymetry was an early beta version of inhouse software.

There are also issues regarding levels between EM710 and HiSAS 1030 bathymetry data. A comparison of this is shown in figure 13. The EM710 data (from surface vessel) and the HiSAS 1030 data seem to follow the same terrain in figure 10. However, there are gaps in the HiSAS 1030 data and level differences between the HiSAS 1030 and the EM 710 data.

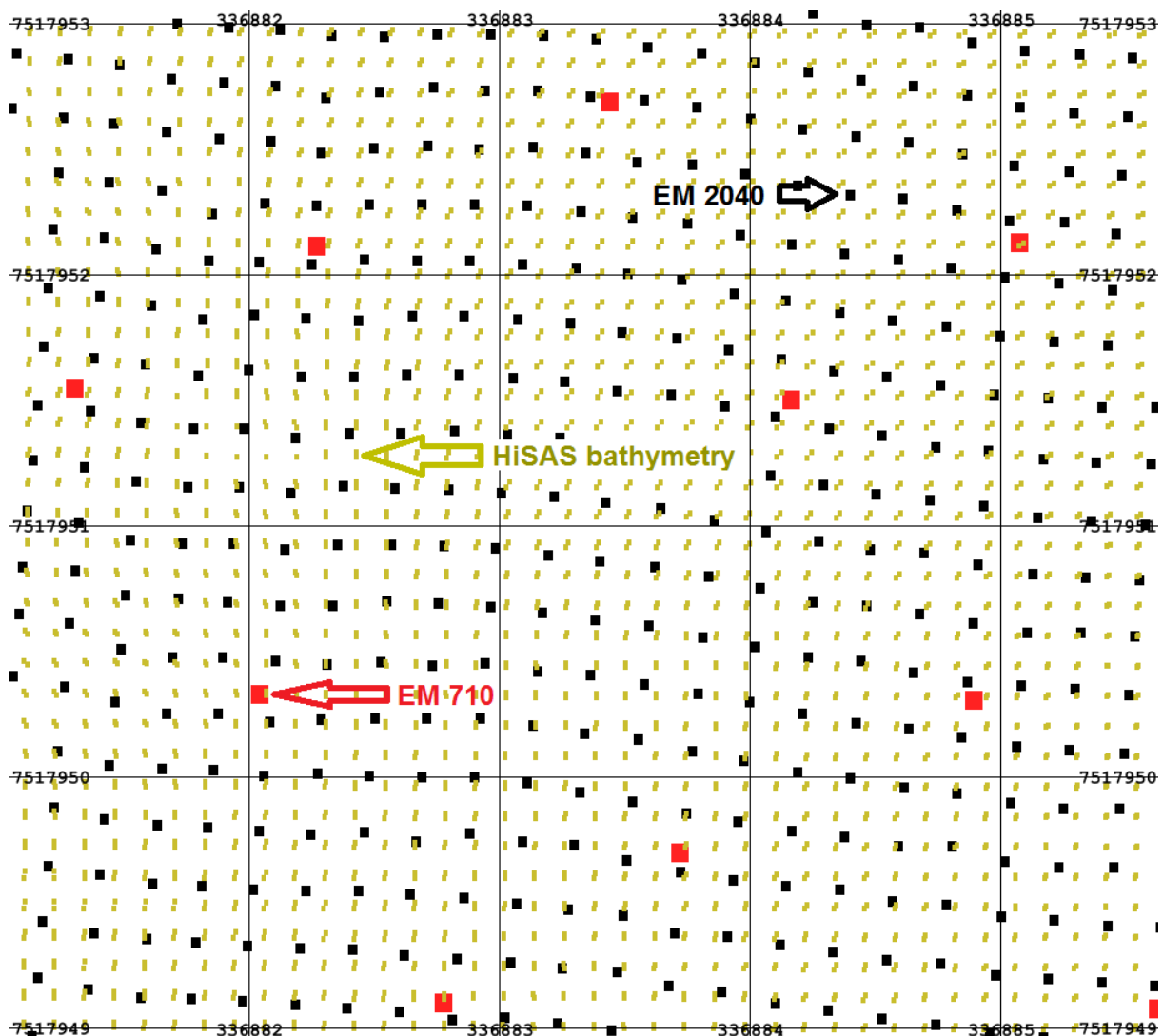


Figure 9. Density of the bathymetry point cloud from HiSAS 1030 (green), EM2040 (black) and EM 710 (red). The mesh is 1 x 1 meter.

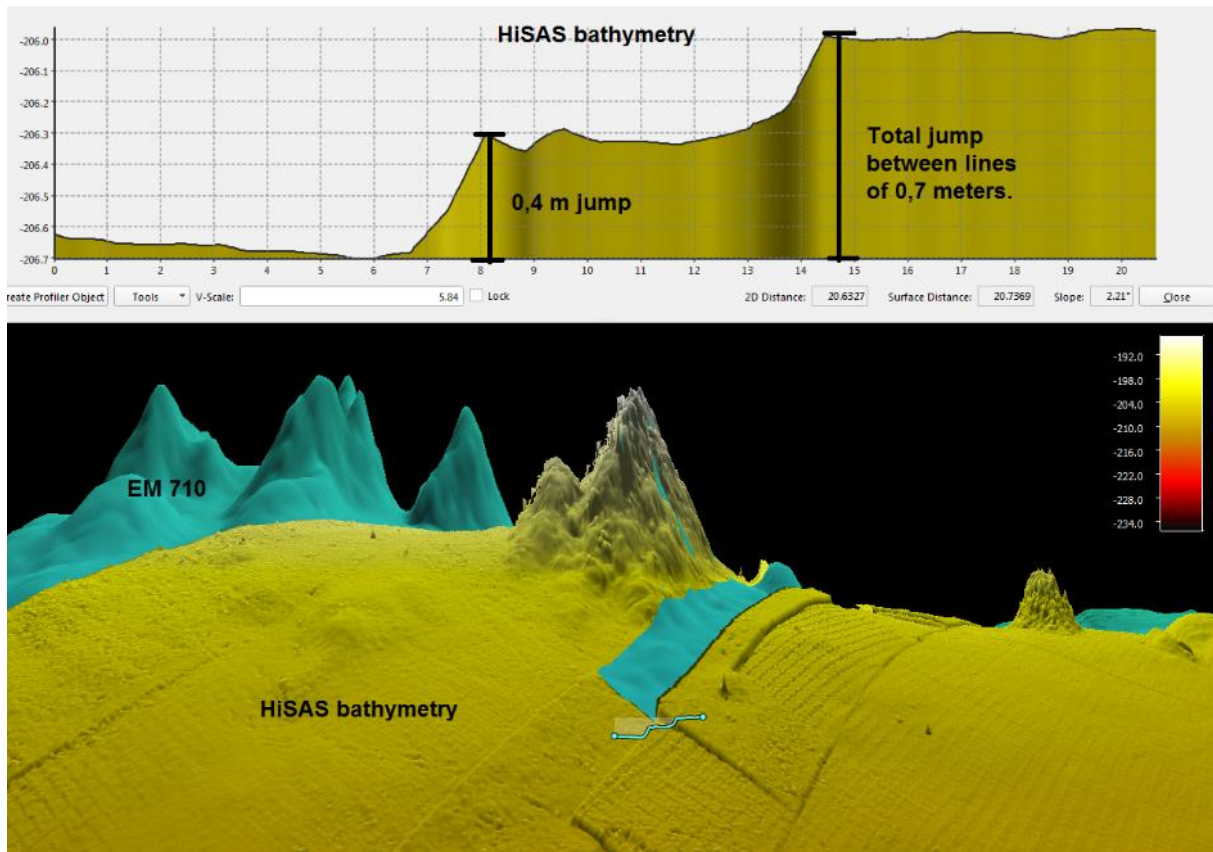


Figure 10. Level difference within HiSAS 1030 data. Upper panel – profile (see lower panel for profile location - light blue line). Lower panel – 3D visualisation.

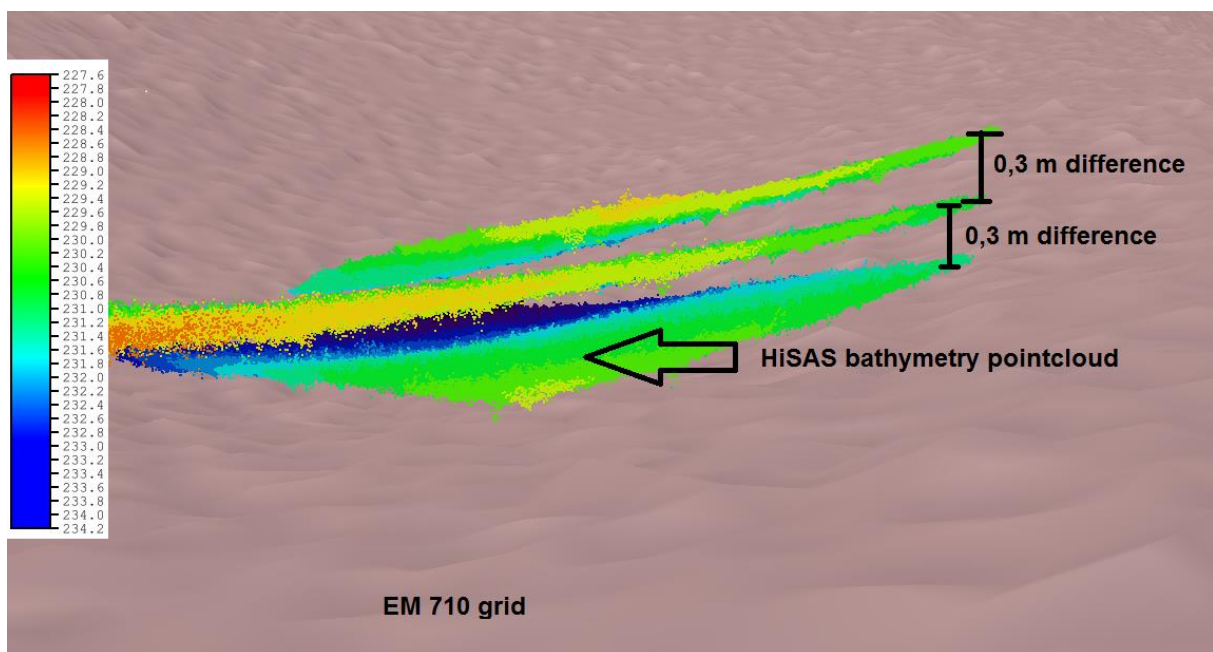


Figure 11. Point cloud of HiSAS 1030 data plotted with EM 710 model (monochrome) in the background. The HiSAS 1030 point cloud data are from three different AUV-lines, and there is a stepwise level difference of 0.3 m per step at a depth of 230 m.



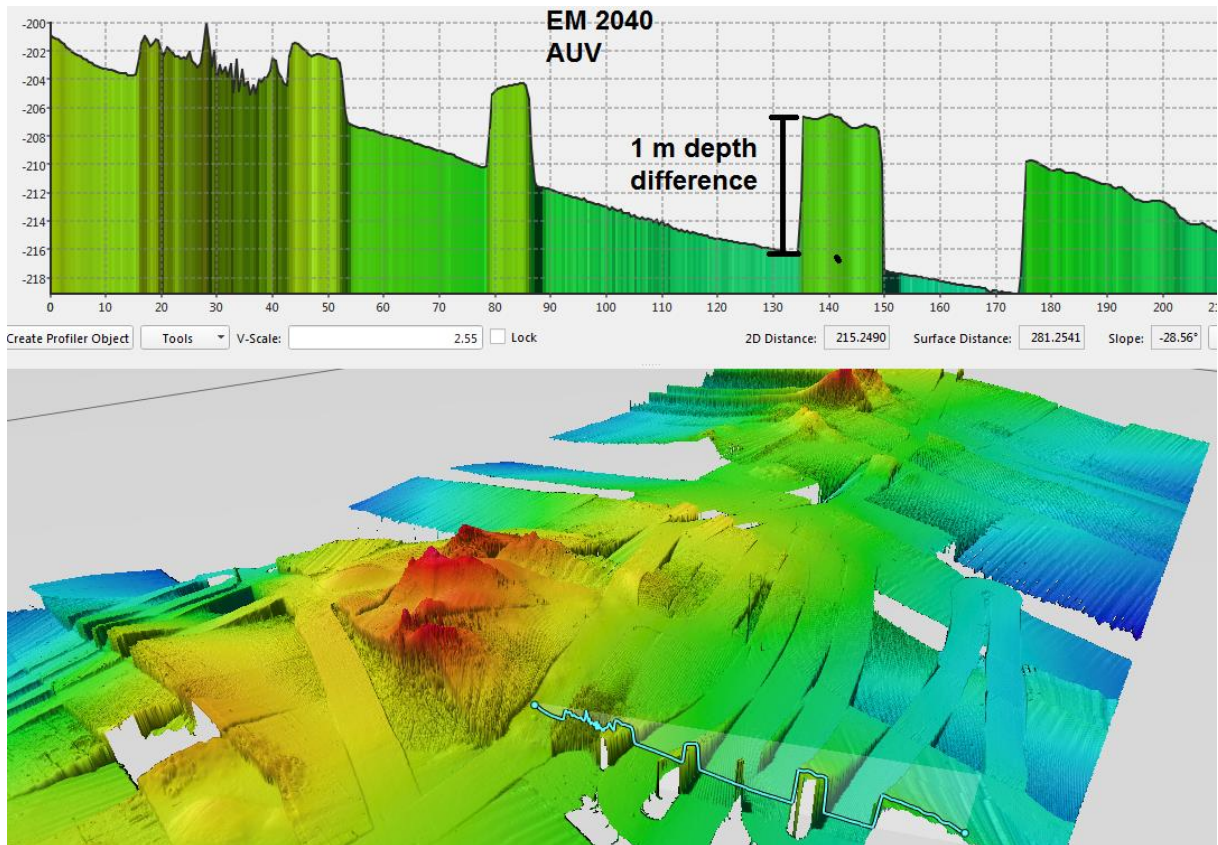


Figure 12. Level difference within EM2040 data (0.5 m grid). Upper panel – profile (see lower panel for profile location - light blue line). Lower panel – 3D visualisation.

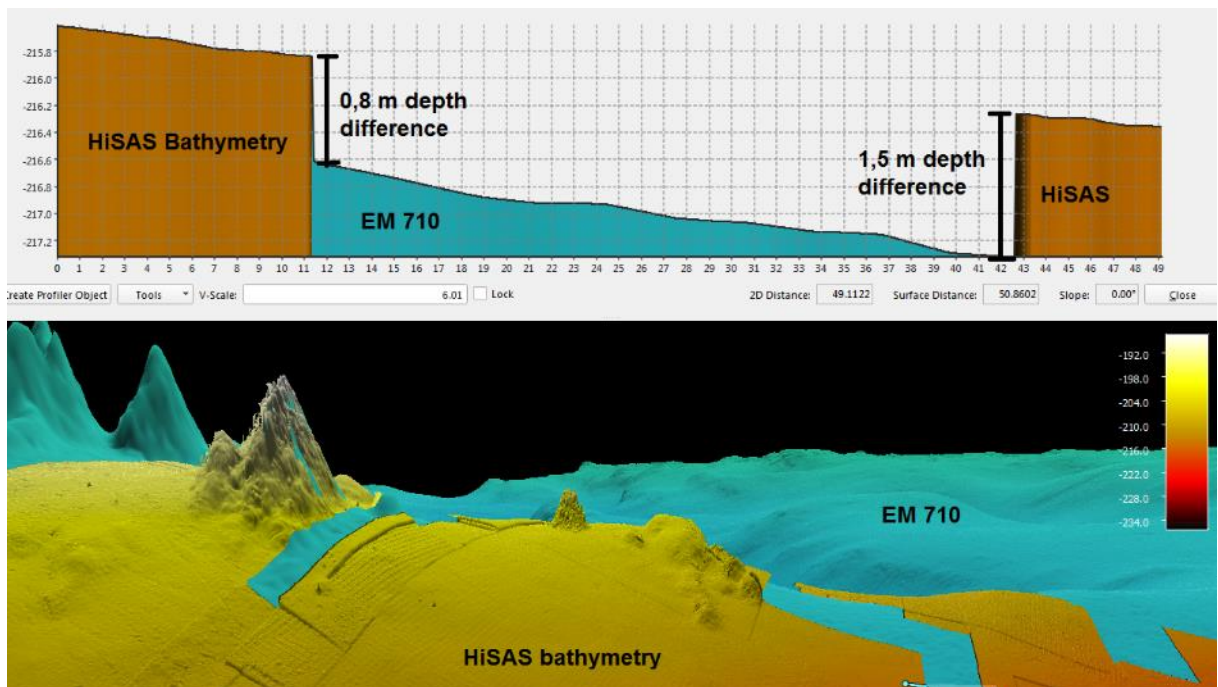


Figure 13. Lower panel: comparison between the bathymetry levels of EM 710 (blue) and HiSAS 1030 (yellow-red). Upper panel: profile showing steps with a magnitude of 0.8-1.5 m.



## 5.2 Visual analysis of bathymetry, backscatter and imagery from EM710, EM2040 and HiSAS 1030

A compilation of bathymetry data and backscatter/sonar imagery data collected with hullborne EM710 multibeam echosounder, and AUV-borne EM2040 multibeam echosounder and HiSAS 1030 sonar is shown in figure 14.

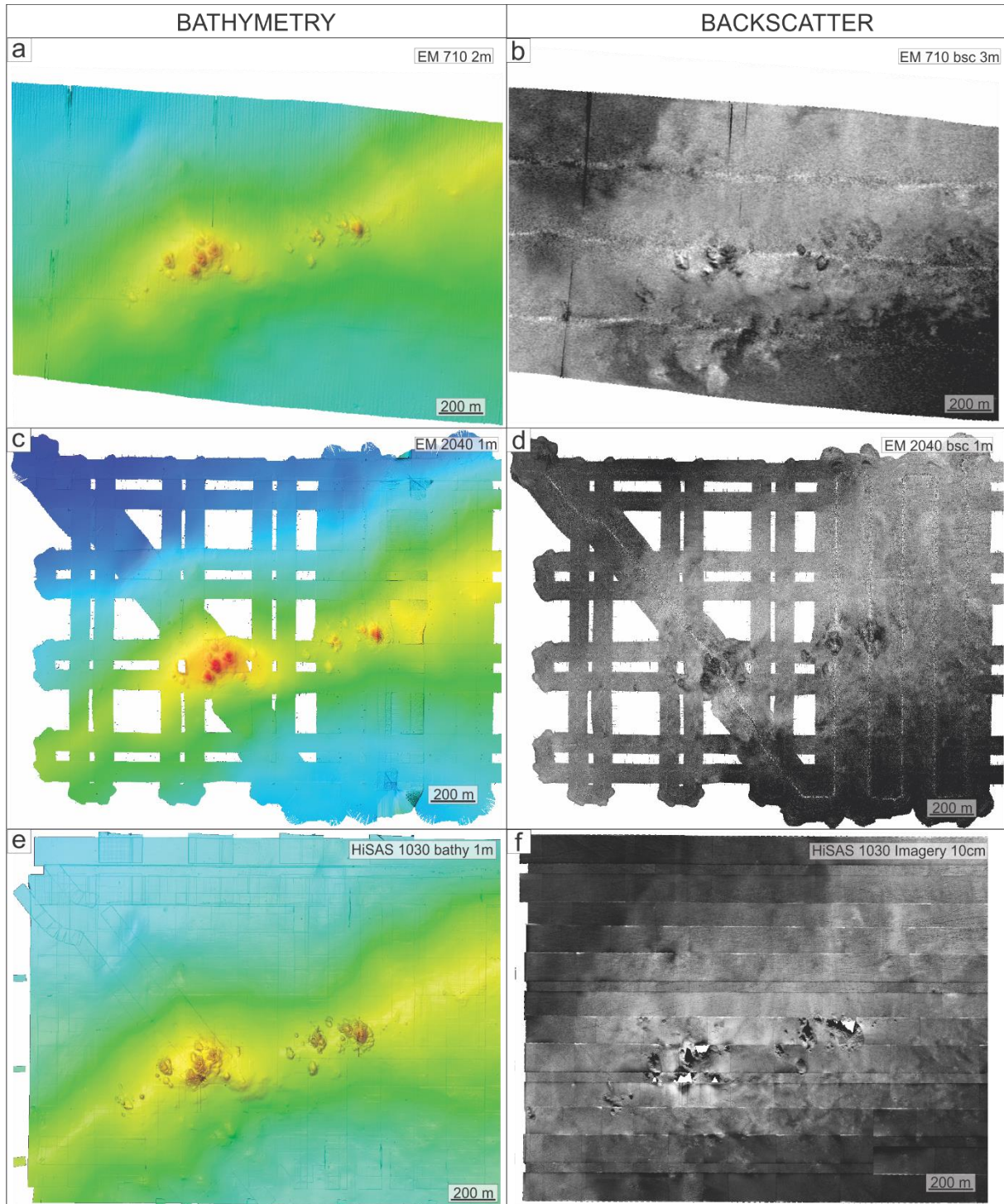


Figure 14. Comparison between data from hullborne EM710 multibeam echosounder from 2015 (a, b), AUV-borne EM2040 multibeam echosounder (c,d) and HiSAS 1030 (e,f).

The EM710 bathymetry data collected in 2015 were processed to a 2 m grid (figure 14a), because a visual inspection of the shaded relief image indicated that this was the maximum resolution that could be extracted from the data. The EM2040 bathymetry data were processed to a 1 m grid (figure 14c), while the HiSAS 1030 data were processed to a 20 cm grid (figure 14e). The grid sizes from EM2040 and HiSAS 1030 data were also selected based on a visual assessment of the maximum resolution possible to achieve from the data sets.

The HiSAS 1030 data were processed to both 20 cm and 1 m grids. The HiSAS 1030 20 cm bathymetry grid shows greater detail, but also high amounts of noise (spikes), as shown in figure 15a. To compare the ability to detect small features like coral blocks and trawl marks, the sonar imagery data is shown in figure 15b. Such small features are clearly seen in the HiSAS 1030 sonar imagery data, while they are present, but far from as obvious as in the HiSAS 1030 bathymetry data. It is also worth noting that bioclastic mounds can be outlined both from bathymetry (morphology) and the sonar imagery intensity. The mounds (outlined with yellow polygons) show up as positive features in the bathymetry (figure 15a). They show up as areas of lower and smoother sonar imagery intensity, with smaller mounds with slightly higher sonar imagery intensity (figure 15b). Coral blocks form parts of the mounds, particularly occupying the southwestern slopes.

The visual resolutions of EM2040 and HiSAS 1030 gridded at 1 m are quite similar (figure 14c and 14e). The objects are somewhat better defined in the EM2040 data. This is partly due to the effect of the very wide swath of the HiSAS 1030, which results in shadows with no data. Another factor is that the same area is covered by many pings, due to the very wide swath. This means that small differences between the different lines, from imperfect correction of flight height or other factors, will result in a more noisy bathymetry data set. This can probably be removed with more extensive processing. The N-S trending artefact lines in both EM2040 and HiSAS 1030 bathymetry images (figure 14c and 14e) give a clear indication of imperfect correction from line to line. It should be noted that the differences are small (10-50 cm), but still large enough to influence the quality.



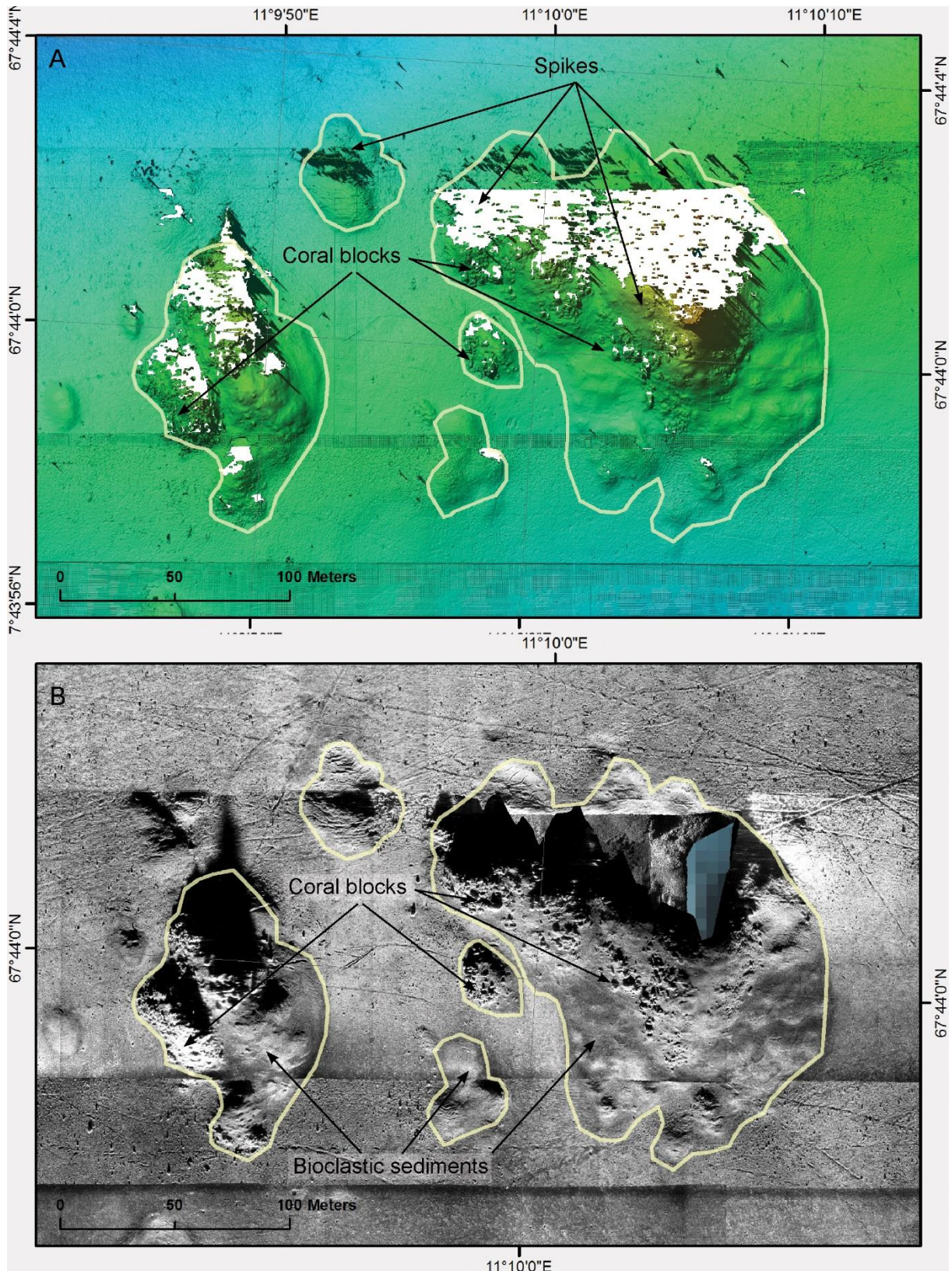


Figure 15. Comparison between HiSAS 1030 bathymetry (A, 20 cm grid) and HiSAS 1030 sonar imagery (B, 10 cm grid). Areas without data (shadows) result from low flight height. Note that coral blocks can be observed both in the bathymetry and sonar imagery data. Yellow polygons show the outlines of bioclastic sediments based on morphology (bathymetry) and backscatter intensity. Trawl marks are clearly visible in the sonar imagery (B), while they are rather faint in the bathymetry (A).

The EM710 backscatter data collected in 2015 were processed to a 3 m grid (figure 14b). The EM2040 data were processed to a 1 m grid (figure 14d), while the HiSAS 1030 data were processed to a 10 cm grid (figure 14f). The EM2040 and HiSAS 1030 grid sizes were selected based on a visual assessment of the maximum resolution possible to achieve from the data. In terms of coverage for EM2040 backscatter, the same effect applies in terms of swath width and line spacing as for bathymetry.

A visual comparison of the backscatter data (figure 14b, 14d and 14 f) from EM710 and EM2040 shows a somewhat higher resolution for the EM2040 data compared to EM710, but the difference is less than expected. One noticeable difference is that some trawl marks may be seen in the EM2040 data, although very faint, while it is not possible to detect these trawl marks in the EM710 data. It should be noted that the trawl marks are far more obvious in the bathymetry data than in the backscatter data. Another noticeable difference is that individual objects sometimes are seen clearly in the EM2040, but not similarly clear in the EM710, and sometimes the opposite situation occurs. This appears to be an effect of where the objects are located in relation to the nadir lines, and line orientation (EM710 - NE-SW, EM2040 mainly N-S).

The difference in resolution between the HiSAS 1030 data on one side, and the EM710 and EM2040 data on the other is far more obvious (figure 16). The objects are diffuse in the EM710 image, while they are crisp and sharply defined in the HiSAS 1030 image. Trawl marks are clearly delineated in the HiSAS 1030 image, while they cannot be seen in the EM710 image.

The difference between EM2040 backscatter and HiSAS 1030 sonar imagery can be seen from figure 17a and 17b, respectively. The EM2040 data are here shown in a 20 cm grid, while the HiSAS 1030 data are in a 10 cm grid. Trawl marks which are just on the edge of detection in the EM2040 data are clearly seen in the HiSAS 1030 data. Objects are defined sharply and much clearer than in the EM2040 data. The latter is partly due to the shadow effect related to the very wide swath of the HiSAS 1030. We anticipate that the real resolution of the EM2040 data is close to 1 m.

The ability of HiSAS 1030 to show tiny details is demonstrated even more clearly in small areas, as in figure 18. Objects less than 100 cm, perhaps down to 50 cm, can be identified. Trawl marks passing between, or crossing bioclastic mounds are confidently identified. Individual small mounds, probably representing *Lophelia* coral blocks can be seen. Rock boulders are also to be seen.

We have also compared backscatter from EM710 processed to 3 m grid, with HiSAS 1030 sonar imagery processed to 10 cm grid, and resampled to a 3 m grid (figure 19). The EM710 backscatter and HiSAS 1030 sonar imagery were levelled as well as possible, in order to provide comparable images. The comparison shows two phenomena. The real resolution is



different, because trawl marks evident in the HiSAS 1030 sonar imagery are not visible in the EM710 backscatter. Secondly, the acoustic response differs. The dynamic range seems to be higher for the HiSAS 1030 sonar imagery, providing a better distinction between areas with high and low intensity. There are also differences with regard to the intensity pattern between the two data sets. We suspect that this is a result of the different frequencies used (EM710 - 70-100 kHz; HiSAS 1030 – 85-115 kHz).

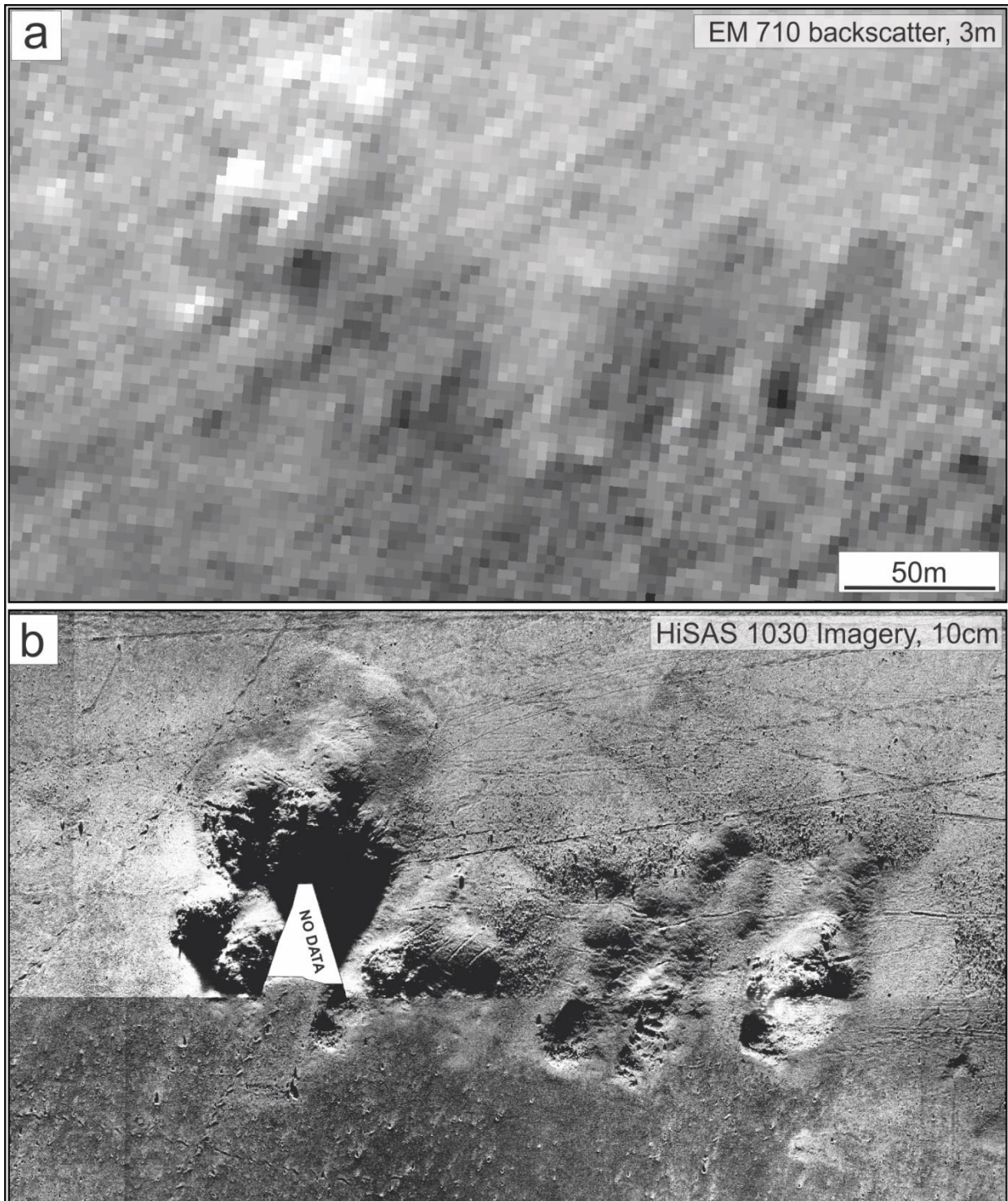


Figure 16. Comparison of EM710 backscatter data (a) and HiSAS 1030 sonar imagery data (b).



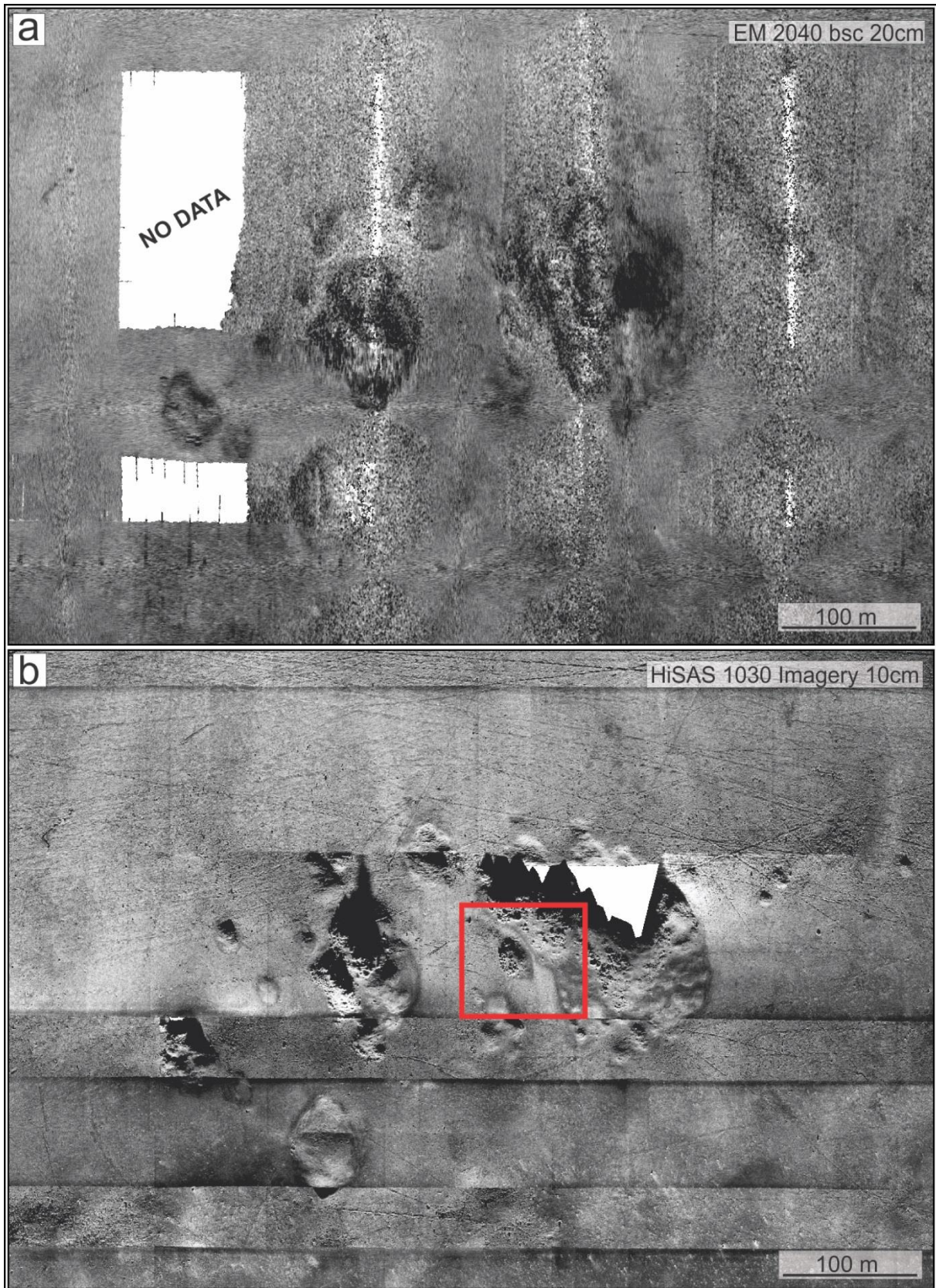


Figure 17. Comparison between backscatter data from (a) EM2040 at 20 cm grid size, and (b) HiSAS 1030 sonar imagery with 10 cm grid size. Red square – location of figure 18.



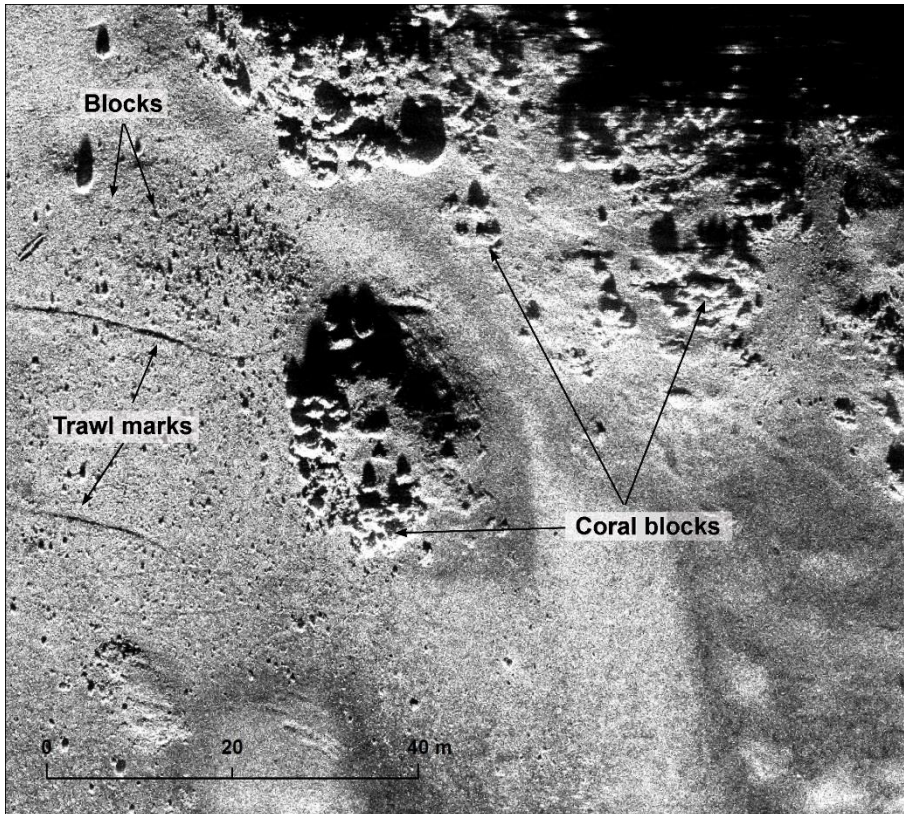


Figure 18. Close-up of the eastern mound (for location, see figure 17), showing HiSAS 1030 data.

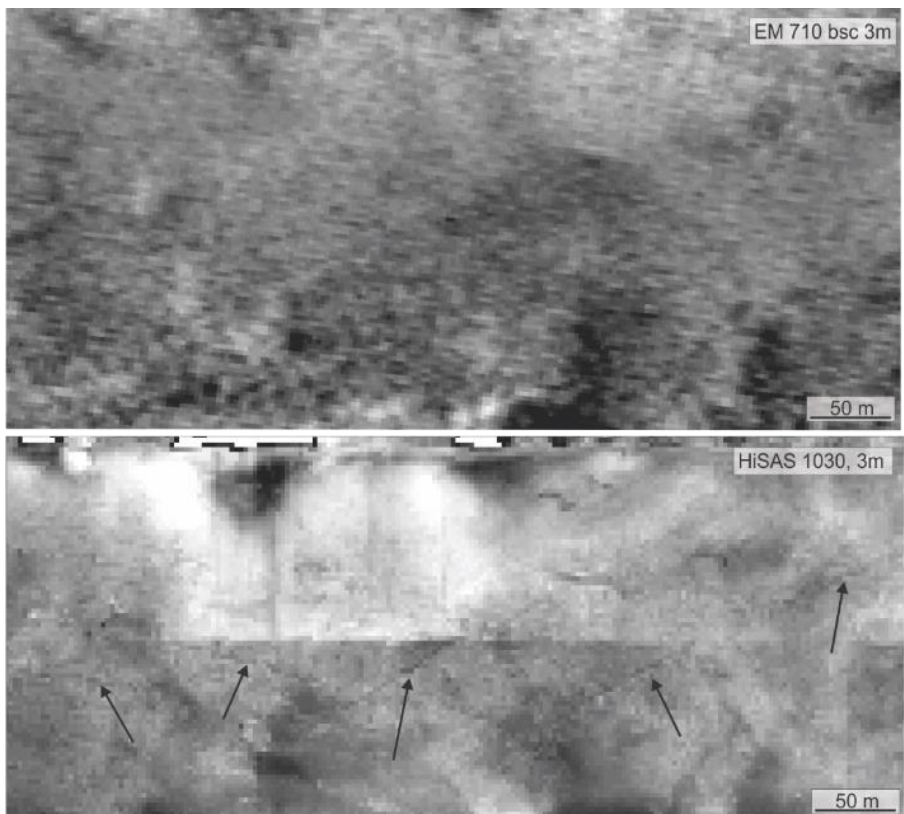


Figure 19. Comparison between EM 710 backscatter (upper panel) and HiSAS 1030 sonar imagery (lower panel). Note trawl marks visible in the lower panel (arrows), and different acoustic response between the two data sets.

### **5.3 Image quality and suitability for geological mapping - Campod and TFish images**

It was not possible to acquire TFish images from exactly the same locations as the Campod video lines because:

- Positioning accuracy of both Campod and TFish is 5-10 m. Campod positioning was with the HiPAP system, while TFish is based on the inertial positioning system of the HUGIN HUS AUV.
- AUV cannot safely climb up or down hills and cannot navigate close to obstacles such as bioclastic mounds.

We have therefore selected representative images from Campod and TFish from different areas, in order to show how the systems perform. In doing this, we have selected a spread from poor images, to average quality images, to good images. This is shown in figure 20 (poor, average, good images). Our experience is that most of the pictures have sufficient quality for seabed sediment classification.

The resolution of the TFish system is in the same range as the Campod HD video system, and the actual pixel size at the seabed is governed by the distance from the seabed to the sensor. In this cruise, we experienced that the AUV seldom were closer to the seabed than 5 m, while the Campod system operates 1.5 m over the seabed (provided very calm sea conditions). In practice the height of the Campod system above the seabed varies considerably, from decimetres to many meters over the seabed, giving poor or no data when the sea condition are rough (but still within the limits of operation).



Campod

TFish

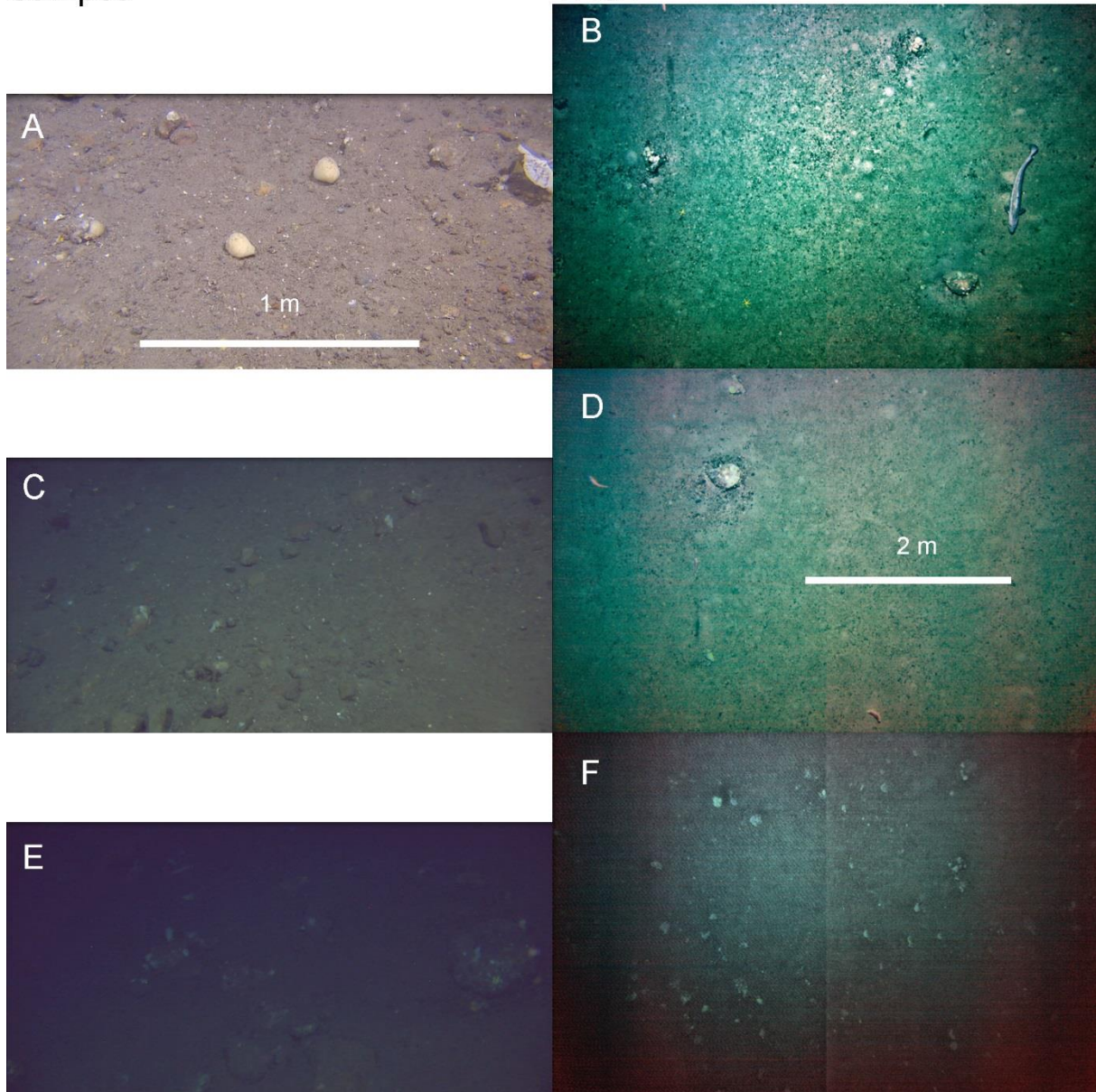


*Figure 20. Examples of images from Campod (A, C and E) and TFish (B, D and F). The upper images have good quality, the middle images have medium quality, while the lower images have poor quality.*

#### **5.4 Geological map production based on Campod versus TFish**

The different modes of operation of the Campod system, which is linked to a towed video platform hanging from a ship (for further details, see Thorsnes et al. 2015), and the TFish system, linked to an AUV, influences the way geological maps are made, and the final products. An example of the difference between the data acquisition strategy using Campod and TFish is shown in figure 21. The tracks of the Campod and the TFish are shown across a ridge where with bioclastic mounds (figure 7). The Campod line (white line) traverses straight uphill, while the AUV has to climb up by going back and forth in lines with less inclination. The time spent by the Campod on a 700 m long video line (including still photography at start

and stop point is 60 minutes, while the time spent by the TFish system is 20-25 minutes, given a speed of 2-4 m/s (average 3 m/s) and a total distance of about 4200 m.

The Campod system gives a continuous record along the single line covering c. 1400 m<sup>2</sup> (the field of view is c. 2 m, provided that the system is positioned 1.5 m above the seabed, and the line is 700 m long. The TFish system collected c. 2300 images covering an area of c. 27 600 m<sup>2</sup> (2300 images, 6 m wide and 4 m high, with 50% overlap). The normal flight height was 5-6 m above the seabed. The colour-coded interpretation of the TFish and Campod images (figure 21) shows that three sediment classes (bioclastic sediments, sandy gravel and sand/gravel/cobbles/boulders) could be recognized with the images from the TFish system, while sandy gravel, gravelly sand, gravel and corals was recorded by the Campod system.

The time needed for a Campod line of 700 m is 60 minutes. The distance covered by an AUV in the same time is 10 800 m, covering a distance which is 15 times longer. The TFish system collects more images covering a larger area, and the HiSAS 1030 sonar imagery and EM2040 backscatter reveal far more detail than the EM710 backscatter. The resulting sediment grain size map reveals far more detail (figure 22). The higher number of seabed images from TFish covering a larger area, together with a more even quality, allows a better classification of the different sediment classes, and a better delineation of spatial distribution.

A striking feature which can be observed on the HiSAS 1030 sonar imagery is the widespread occurrence of trawl marks, particularly close to the bioclastic mounds/coral reefs. An example of this shown in figure 23.



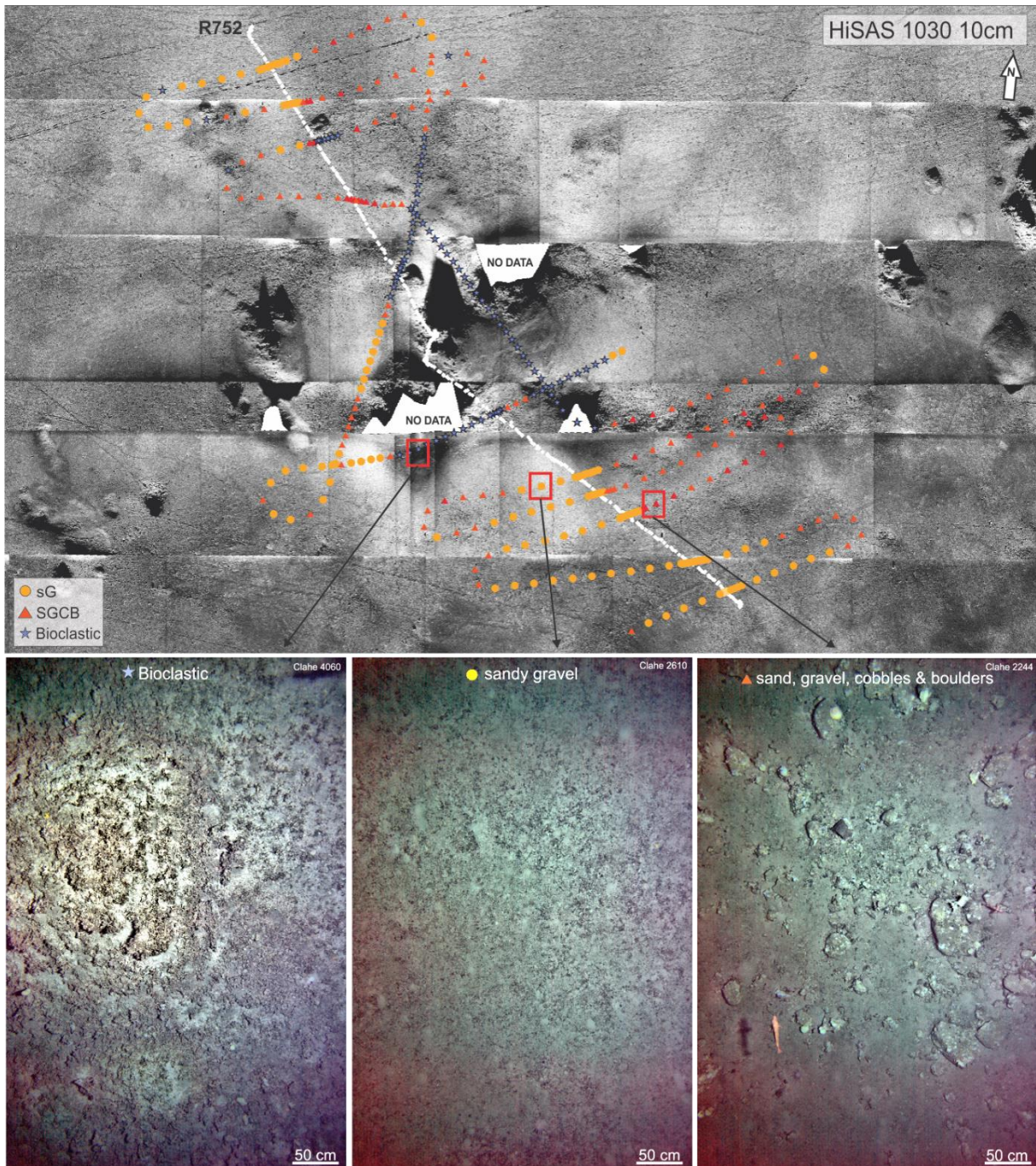


Figure 21. HiSAS 1030 backscatter (10 cm grid size) with video track line (white) and classified TFish images (coloured symbols, see legend on image).

Grain size analysis from MAREANO

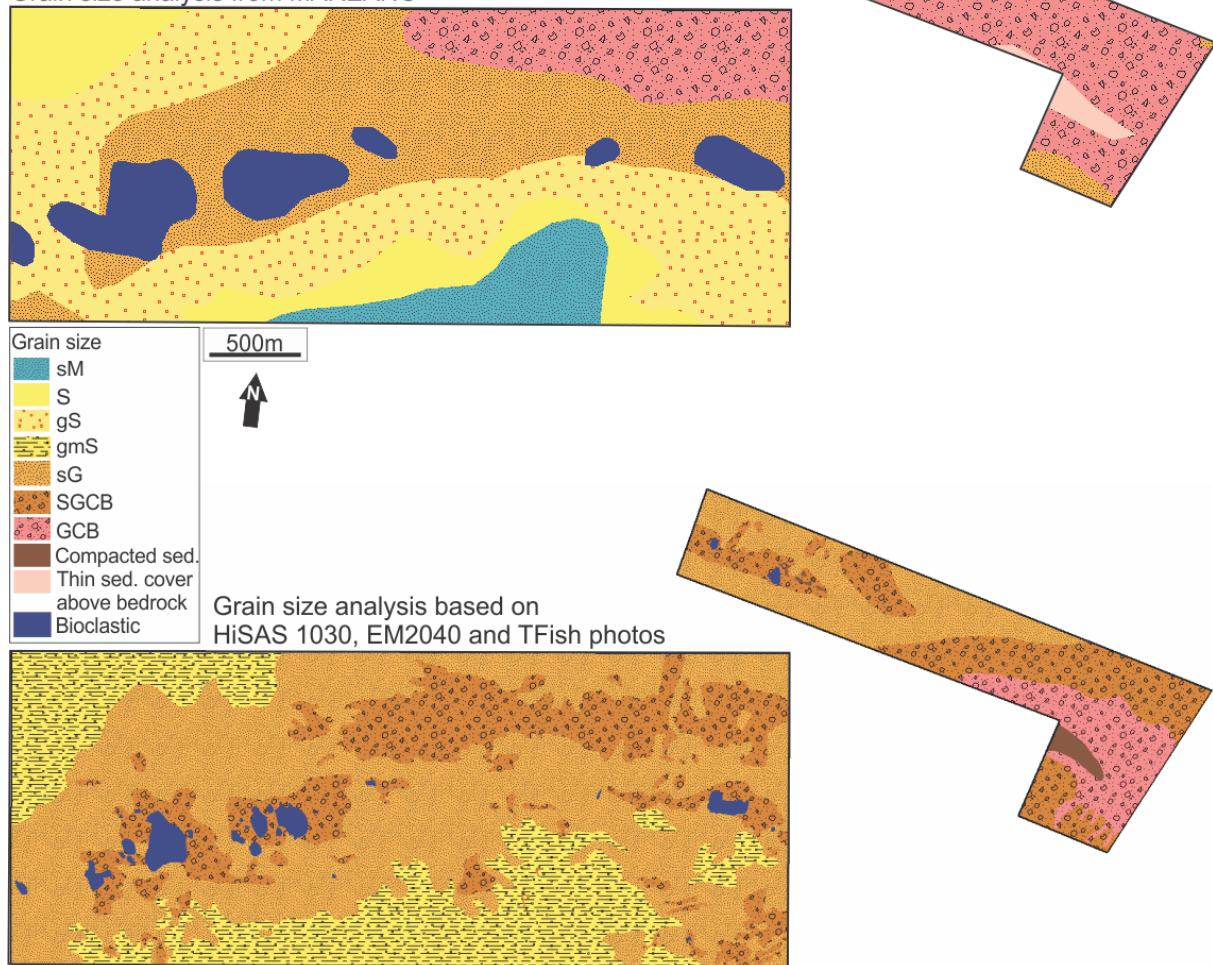


Figure 22. Comparison between grain size sediment map based on EM710 data and Campod videos (upper part) and HiSAS 1030, EM2040 and TFish (lower part). Note that the map extent has been delimited to the areas with EM2040 and/or HiSAS 1030 coverage. Grain size classes: SM – sandy mud, S – sand, gS – gravelly sand, gmS – gravelly muddy sand, sG – sandy gravel, SGCB – sand, gravel, cobbles and boulders.



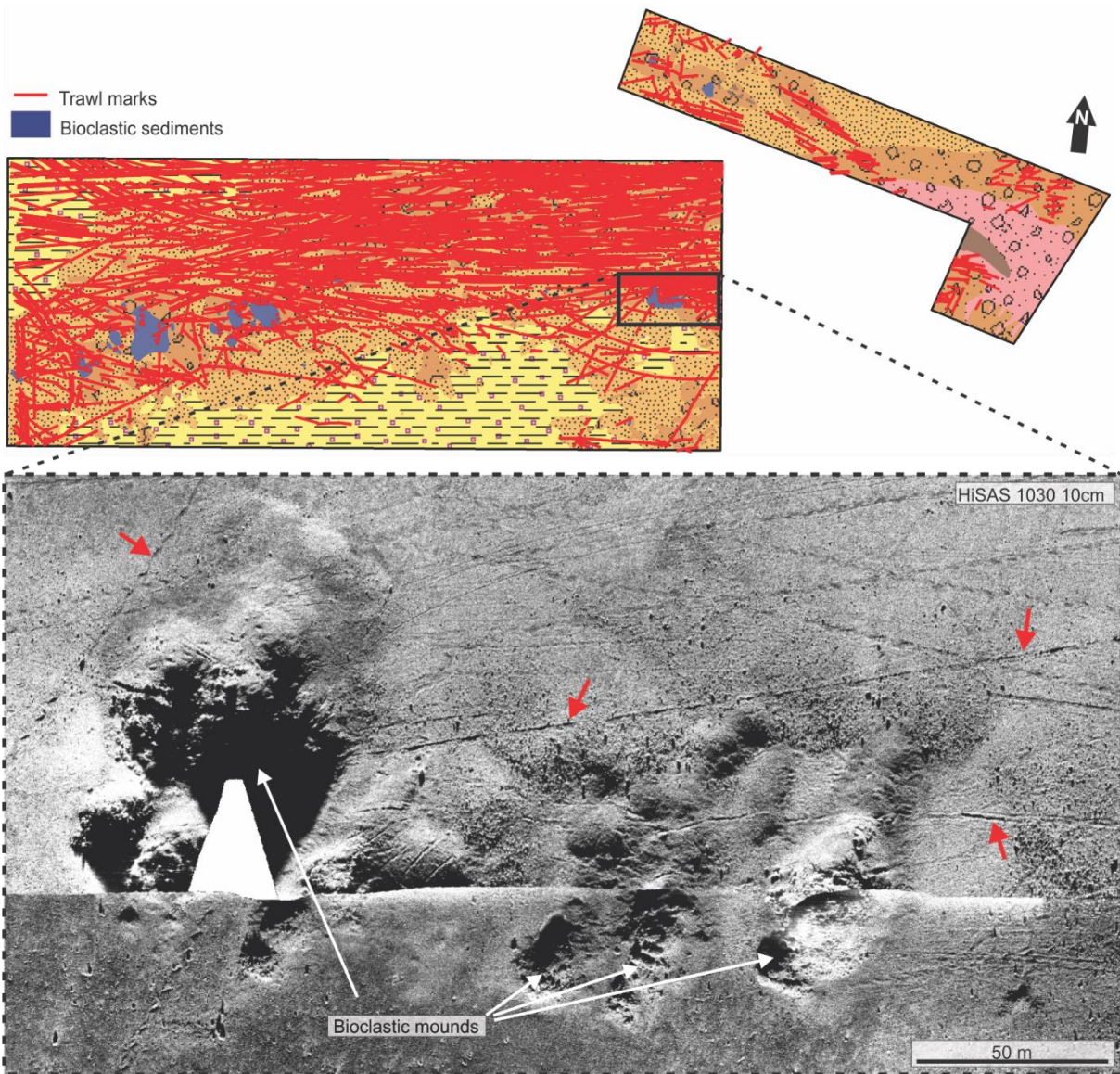


Figure 23. Upper panel: same map as in figure 22, with trawl marks overlain. Lower panel: spatial distribution of trawl marks (indicated by red arrows) close to the bioclastic mounds/coral reefs, HiSAS 1030 imagery, 10 cm grid size.

## 6. COMPARISON OF SPECIES COMPOSITION AND BIODIVERSITY BETWEEN AUV STILLS AND CAMPOD VIDEOS

Comparison of species composition and biodiversity between AUV stills and Campod videos were made for three video lines (R751, R752, and R796). This comparison is based on full video records covering around 700 m distances along the seabed and a variable number of stills from the three AUV transects (72-156 images, Table 5). The results from video analyses of the stations surveyed by Mareano are part of the same data set as have been used for identification of general biotopes ([www.mareano.no](http://www.mareano.no)). The values in table 5 represent total number of observed individuals or colonies. To study the effect of variable number of stills, curves of cumulative number of taxa were made for results from the stills from the three stations (figure 24).

**Table 5. Sum of individuals and colonies of identified and unidentified species from still images captured by AUV and from videos recorded by Campod (Cam), at video lines R751, R752, and R796.**

	R751		R752		R796		AUV only	Cam only	Both
	AUV	Cam	AUV	Cam	AUV	Cam			
Species No of images:	120		72		156				
Actiniaria	3	2			5	2			x
Actiniaria; dark	5				2		x		
Actiniaria; orange	3				3	1			x
Actiniaria; pink	7	5	1	14	20	25			x
Actiniaria; white	1	3	8	3	4	4			x
Actiniaria purple						1		x	
Actiniaria red				1				x	
Antedonacea				1				x	
Antho dichotoma		3						x	
Aplysilla sulfurea		2		3		12		x	
Ascidia transparent				3				x	
Asconema setubalense		1						x	
Asteroidea					1		x		
Axinella infundibuliformis	1	12		12		1			x
Axinellidae						3		x	
Bivalvia				1				x	
Bolocera tuediae	58	16		3					x
Bonelliidae	1	1			4	24			x
Brachyura					1		x		
Brachiopoda		11		14		1		x	
Brosme brosmes				1	1				x
Bryozoa calcareous branched				17				x	



Bryozoa encrusting		6					x	
Burrow; big	2		128		13		x	
Burrows small		6	10	58	10			x
Caridea				3			x	
Ceramaster granularis				2	1	1		x
Cerianthidae	29	9	9		26	5		x
Cerianthidae; dark					1		x	
Cerianthidae purple				10			x	
Chimaera monstrosa	1					1		x
Didemnidae		1					x	
Drifa glomerata		75					x	
Echinoidea regular				1	1			x
Echinus sp		4				1	x	
Echiura				98			x	
Gadidae		10		5	1	7		x
Gadiculus argenteus				1			x	
Gadus morhua		1		2			x	
Gastropoda				3			x	
Geodia atlantica	1	1						x
Geodia barretti		3				1	x	
Geodia macandrewii		1					x	
Geodia sp		2				1	x	
Henricia sp.; yellow	4	9	6	27	31	15		x
Holothuroidea	2						x	
Horneridae		14				1	x	
Hydrozoa		1		33			x	
Hydrozoa bush		3					x	
Hymedesmia paupertas			2	47	1			x
Lebensspuren tracks					1		x	
Lithodidae			1				x	
Molva molva			1	5		1		x
Munida sp.	1	72	2	213	1	7		x
Mycale lingua		4	5	86	1	26		x
Nemertea					1	1		x
Nephtheidae	850	33						x
Ophiuroidea		6		4		2	x	
Pachycerianthus			3				x	
Paguridae		1					x	
Pandalidae		2					x	
Paragorgia arborea				44		1	x	
Parastichopus tremulus	28	17	1	20	31	17		x

Phakellia sp.	65	109	144	66	284	57			x
Phakellia sp.; fragment					1		x		
Phycis blennoides	1	7		4	1	4			x
Pollachius virens		12		1				x	
Polychaeta Errantia						1		x	
Polychaeta tube						2		x	
Polymastia				1				x	
Poraniidae					2	1			x
Poraniomorpha				1				x	
Porifera bat				7				x	
Porifera big; white		1	2						x
Porifera branched				1				x	
Porifera dirtyyellow		8		1		11		x	
Porifera encrusting	3424	830	1439	317	3528	267			x
Porifera encrusting bluegrey				26				x	
Porifera encrusting brown				1				x	
Porifera encrusting green				1				x	
Porifera encrusting grey				6				x	
Porifera encrusting; orange	1			74	40				x
Porifera encrusting; purple	4				6		x		
Porifera encrusting; white	76		388	130	657				x
Porifera encrusting; yellow	43	51	134	190	482	62			x
Porifera fan small					8		x		
Porifera medium	325		4		131		x		
Porifera medium; white	40		356	15	427				x
Porifera medium; yellow		1		10	1				x
Porifera medium yellow irreg				1				x	
Porifera white		26				7		x	
Porifera yellow						7		x	
Porifera small					332		x		
Porifera small; white			509		3		x		
Porifera small; yellow					7		x		
Primnoa resedaeformis				48				x	
Prosobranchia		2				1		x	
Protanthea simplex				119				x	
Quasilina cf		1						x	
Reteporella beaniana		8		3	9	2			x
Sabellidae		1		2				x	
Sebastes sp.	24	22	35	49	103	4			x
Selachii (Shark)	1						x		
Serpulidae		16		14	1				x

Solaster endeca	1						x		
Stichastrella rosea				1				x	
Stryphnus ponderosus						1		x	
Stylocordyla				11				x	
Stylocordyla Hyalonema				1				x	
Teleostei	30		35		54		x		
Tentorium semisuberites		1						x	
Trisopterus sp		6		32				x	
Unidentified; black					5		x		
Unidentified; red					1		x		
Unidentified; white			1150				x		
<b>Sum</b>	30	50	24	60	45	40	22	57	36

In total, for both gears 115 taxa were identified. Half of the taxa were identified only from the Campod videos, whereas 19% of the taxa were only observed on the AUV images. 31% of the taxa were observed by both gears. Except for line R796, many more taxa were observed on the video records than on the stills. At R796, 45 taxa were observed on the stills, and 40 on the video records. Based on the shape of the cumulative species curves (figure 24), the number of images is not sufficient to capture the full diversity of species, but is sufficient to provide comparative results on species diversity between AUV transects (based on a criterion where a 10% increase in sampling size leads to less than 10% increase in number of species/taxa). Lines R751 and R752 have similar curves, whereas R796 differs with both a steeper initial increment and faster flattening at a higher level. How well the results from these stills are for characterizing biotopes is a different question. The results presented in table 5 indicate that several large and characteristic species, such as the sponge *Aplysilla sulfurea*, were not documented in the stills at any of the stations, even though common on all video lines. The image quality of the stills makes it more difficult to identify organisms, e.g. fishes (Teleostei) to species level than the images from Campod. This implies that the species compositions based on AUV stills will be of lesser use for defining biotopes than higher quality images from Campod.

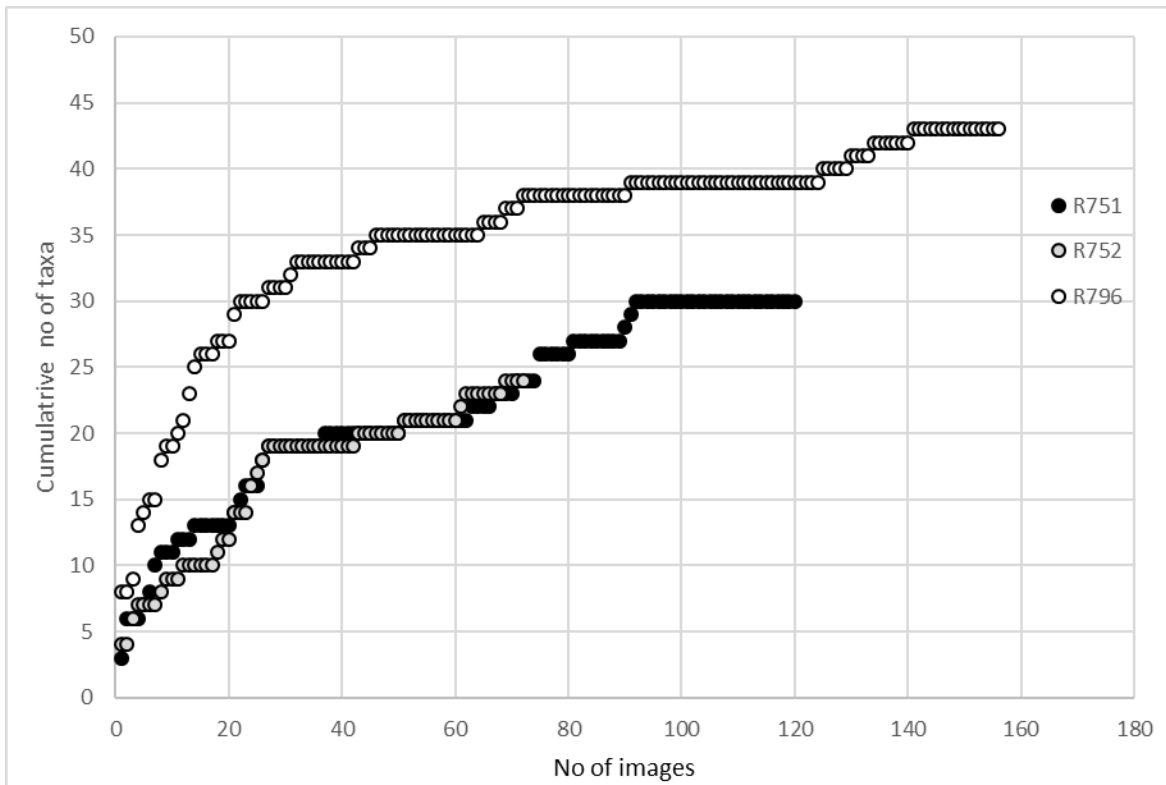


Figure 24. Cumulative number of taxa (identified and unidentified species) with increasing number of still images from the AUV.

It should be noted that a similar comparison (Morris et al. 2014) of optical imaging using a towed video platform (WASP) and an Autosub 6000 AUV with two 5 Megapixel cameras in water depths between 4600 and 4900 metres in the NE Atlantic Ocean SW of UK concluded that comparison of taxon richness and diversity across techniques are complex and encompass a number of uncontrolled factors. They found nevertheless that the Autosub 6000 method uniformly produced 30% to 60% higher estimates than the WASP towed camera and trawl data for the same sample size (as number of individuals).



## **7. USING AUV-BASED SENSORS FOR CORAL MONITORING**

Clearly, images provided using HISAS provide more details about the local topography and spatial distribution of coral reef structures (build-ups and large colonies). The images do not show whether the colonies are dead or alive, but are a powerful tool to delineate the extension of individual reefs. The status of the reefs (living, dead, damaged) can be indicated by stills taken from the AUV, but without a full visual coverage of the same structures, encounters only of dead corals cannot exclude the possibility of occurrences of live patches. Marks from bottom trawl are clearly visible on HISAS images (figure 23) and can be of great value for assessing the extent of damage to coral reefs (e.g. as a background for interpreting visual inspection information). It should be noted that trawl marks also can be detected in the EM2040 data, but with a lower sensitivity.

## 8. CONCLUSIONS

The test was done during a five-day cruise in October 2015. There were several issues reducing the amount and quality of data from the cruise. Strong winds and accompanying waves meant that one of the reserve areas had to be used, and there was only limited time available for the priority areas. The waves prevented grab sampling to verify the acoustic and optical data. The EM2040 transponder was mounted incorrectly, giving severe delays in data delivery and reduced data quality. The optical system (TFish) had several issues, and the equipment is no longer in use by FFI. Nevertheless, the test has given very valuable experience, and demonstrates a clear potential for using AUV in future MAREANO mapping, with some limitations.

The bathymetry collected by the various sources display great differences in data density, from relatively sparse density of the hull mounted EM710, to the dense data collected by the HiSAS 1030. HiSAS 1030 data collected at a flight height of 20-25 meters has a data density of up to 3 times that of bathymetry collected with EM2040 at the same height, and almost 200 times the density of the surface-based EM710-data. The difference in data density between EM2040 and HiSAS 1030 is 180 points to 760 points respectively. That means HiSAS 1030 bathymetry has 4 times more data than EM2040.

In general, data from the HUGIN is following the terrain from the EM710 data, hence there is some degree of consistency between the data. However, level differences in the data sets from the three sensors, and ambiguities within each sensor dataset make it difficult to achieve a fully consistent combination/comparison of data. In some cases, HiSAS 1030 bathymetry data have several layers with different levels. EM 2040 data have very noticeable differences between lines. Level differences in the data from both EM2040 and HiSAS 1030 are probably a result of a lack of navigation correction and insufficient processing of the data. Combined with the 180° error of the EM2040 equipment, this makes a comprehensive assessment of the resulting data difficult.

Data processing is not evaluated in this report. Data can probably be improved if processing steps are quality assured and documented. Sound velocity is in general a significant source of uncertainty in bathymetry data, but has not been evaluated.

An important operational concept of HUGIN is to combine HiSAS 1030 and EM2040, but this is only done at a specific height above the seafloor. In trials done by other HUGIN operators results show a consistent dataset combining EM2040 and HiSAS 1030 bathymetry.

Backscatter from the EM710 (surface) and EM2040 (AUV) differs, with the latter having higher resolution. The difference is surprisingly small. In contrast, the imagery from HiSAS 1030 (AUV) reveals details which are several orders of magnitude better than EM2040 (AUV). The HiSAS 1030 imagery is excellent for detecting e.g. trawl marks, and individual coral heads. This means that coral reef damage may be observed on the HiSAS 1030 imagery.

The images from the TFish colour imagery system are suitable for sediment classification. Due to the stability of the platform, the quality is more even than footage from towed platforms. It is a challenge to fly the AUV sufficiently close to the seabed, particularly in irregular terrain, and this may affect the image quality adversely. AUV-based optical systems can collect data from distances which are c. 15 times higher than optical systems mounted on towed platforms. This allows for more optical observations covering a larger area within the same time frame.

Geological map production based on AUV-data allows far more detailed sediment maps to be produced. The main reason for this is very detailed HiSAS 1030 imagery, but also better coverage from the AUV-mounted optical system. It is important to keep in mind that the time needed for producing these more detailed maps will increase considerably.

Biotope maps of the same standard as normal MAREANO maps using the Campod system cannot be produced with the imagery from the TFish system because the number of images was insufficient to capture full diversity, but it is sufficient to provide comparative results on species between the AUV transects. It is worth noting that other studies employing AUV-based optical systems favour such systems instead of towed video systems.

For coral monitoring, HiSAS 1030 imagery provide detailed information on trawl marks and can be of great value for assessing the extent of damage to the coral reefs. HiSAS 1030 imagery does not provide information on whether the colonies are dead or alive. AUV stills can be useful, but it is difficult to get sufficient coverage with AUV because of manoeuvring limitations inherent in present day AUV systems.

The use of autonomous vessels as platforms for acoustic and optical data collection has a clear potential in MAREANO, but the system which was used in this test was not sufficiently mature for regular MAREANO data collection.

The bathymetry and backscatter data provided by the AUV-mounted EM2040 were sub-optimal due to the technical issues with erroneous mounting. The data have higher detail than the hull mounted EM710 data, but it is impossible to fully evaluate the difference due to the mounting problems and possibly limited post-processing. It is therefore necessary to take into consideration results from surveys which have not had similar problems. For deep sea surveys in the Norwegian Sea, the use of AUV-mounted systems is necessary if sufficient resolution for sediment and biotope mapping is to be achieved.

The HiSAS 1030 imagery has demonstrated ability to provide the basis for detailed sediment mapping, and assessments of e.g. trawl intensity and coral reef damage. For regional mapping, the provided detail is in excess of what is necessary but having the possibility to collect HiSAS 1030 data from key areas would be beneficial in order to understand processes and features.

AUV-based optical systems give far larger areal coverage but the quality of the optical system used (TFish) combined with the flight height prevented good data quality for MAREANO standard biotope map production. The quality was sufficient for sediment map production. It is expected that newer systems developed since 2015 combined with lower flight height may overcome these problems, and there is a need to evaluate more recent and better systems.

## **9. APPENDIX**

### 9.1 HUGIN family

[https://www.km.kongsberg.com/ks/web/nokbg0397.nsf/AllWeb/A6A2CC361D3B9653C1256D71003E97D5/\\$file/HUGIN\\_Family\\_brochure\\_r2\\_lr.pdf?OpenElement](https://www.km.kongsberg.com/ks/web/nokbg0397.nsf/AllWeb/A6A2CC361D3B9653C1256D71003E97D5/$file/HUGIN_Family_brochure_r2_lr.pdf?OpenElement)

### 9.2 Navlab

<https://www.km.kongsberg.com/navlab>

### 9.3 HUGIN payload description

<https://www.sut.org/wp-content/uploads/2014/09/USB-07.-Grant-Rawlinson-HUGIN-Payload-Sensors-5-Minute-Presentation.pdf>

### 9.4 HISAS 1030

[https://www.km.kongsberg.com/ks/web/nokbg0397.nsf/AllWeb/86E9FFB43569CDEEC12576B9006D75C7/\\$file/HISAS\\_1030\\_brochure\\_v1\\_lowres\\_v2.pdf?OpenElement](https://www.km.kongsberg.com/ks/web/nokbg0397.nsf/AllWeb/86E9FFB43569CDEEC12576B9006D75C7/$file/HISAS_1030_brochure_v1_lowres_v2.pdf?OpenElement)

### 9.5 Combined HiSAS 1030 and EM2040

[https://www.iho.int/mtg\\_docs/rhc/EAtHC/EAtHC14/KongsbergMarine\\_14CHAtO\\_KM\\_presentation\\_2.pdf](https://www.iho.int/mtg_docs/rhc/EAtHC/EAtHC14/KongsbergMarine_14CHAtO_KM_presentation_2.pdf)



## 10. REFERENCES

Morris, K. J. 2014: A new method for ecological surveying of the abyss using autonomous underwater vehicle photography. *Limnology and Oceanography: Methods* 12, 795-809.

Thorsnes, Terje; van Son, Thijs Christiaan; Dolan, Margaret F.J.; Gonzalez-Mirelis, Genoveva; Baeten, Nicole; Buhl-Mortensen, Pål; Bjarnadottir, Lilja Run; Hodnesdal, Hanne; Bellec, Valerie 2015: An assessment of scale, sampling effort and confidence for maps based on visual and acoustic data in MAREANO. NGU report 2015.043, 97 pp.

Wynn, R. B. et al. 2014: Autonomous Underwater Vehicles (AUVs): Their past, present and future contributions to the advancement of marine geoscience. *Marine Geology* 352, 451-468.



GEOLOGICAL  
SURVEY OF  
NORWAY

· NGU ·

Geological Survey of Norway  
PO Box 6315, Sluppen  
N-7491 Trondheim, Norway

Visitor address  
Leiv Eirikssons vei 39  
7040 Trondheim

Tel (+ 47) 73 90 40 00  
E-mail [ngu@ngu.no](mailto:ngu@ngu.no)  
Web [www.ngu.no/en-gb/](http://www.ngu.no/en-gb/)